Electronic Supplementary Material (ESI) for Chemical Communications
This journal is © The Royal Society of Chemistry 2012

Electronic Supplementary Information

Novel [2]pseudorotaxanes constructed by self-assembly of bis-urea-functionalized pillar[5]arene and linear alkyl dicarboxylates

Qunpeng Duan, Wei Xia, Xiaoyu Hu, Mengfei Ni, Juli Jiang, Chen Lin, Yi Pan and Leyong Wang*

Key Laboratory of Mesoscopic Chemistry of MOE, Center for multimolecular Chemistry, School of Chemistry and Chemical Engineering, Nanjing University, Nanjing 210093 (China). Fax: +86 025 83597090; Tel: +86 025 83592529; E-mail: lywang@nju.edu.cn

This journal is © The Royal Society of Chemistry 2012

1. *Materials and methods*

All reagents were commercially available and used as supplied without further purification. Compound **1**[S1] and **G5**[S2] were prepared according to the published procedures. NMR spectra were recorded with a Bruker Advance DMX 300 spectrophotometer or a Bruker Advance DMX 400 spectrophotometer with use of the deuterated solvent as the lock and the residual solvent or TMS as the internal reference. Low-resolution electrospray ionization mass spectra (LR-ESI-MS) were obtained on Finnigan Mat TSQ 7000 instruments. High-resolution electrospray ionization mass spectra (HR-ESI-MS) were recorded on an Agilent 6210 TOF LCMS equipped with an electrospray ionization (ESI) probe operating in positive-ion mode with direct infusion.

2. *Synthesis of compound **H**.*

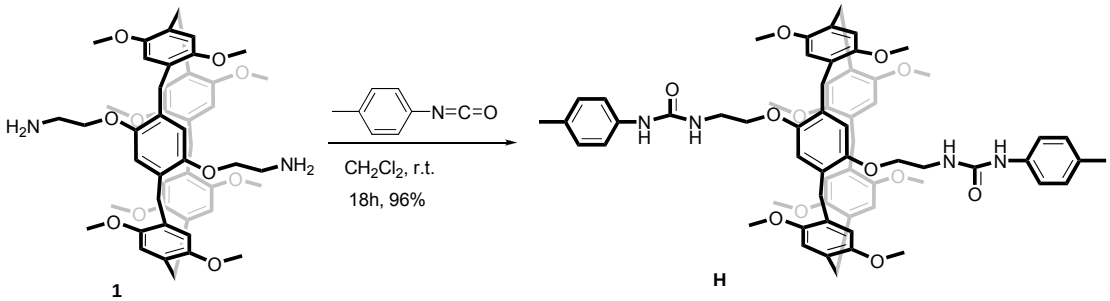

Scheme S1. Synthesis of bis-urea-functionalized pillar[5]arene host (**H**).

To a solution of compound **1** (0.95 g, 1.17 mmol) in dry CH_2Cl_2 (150 mL) was added *p*-tolyl isocyanate (0.47 g, 3.51 mmol) under an argon-gas atmosphere. After stirring at room temperature for 18 h, the solvent was removed and the residue was purified by silica gel chromatography (CH_2Cl_2/MeOH, 200:1) to afford compound **H** as a white solid (1.21 g, 96 %). mp 136-138 ºC. The ^{1}H NMR spectrum of **H** is shown in Figure S1. ^{1}H NMR (300 MHz, DMSO-d_6) δ (ppm): 8.45 (s, 2H), 7.28 (d, J = 8.1 Hz, 4H), 7.03 (d, J = 8.2 Hz, 4H), 6.86 (s, 2H), 6.76-6.81 (m, 8H), 6.37 (t, J = 5.2 Hz, 2H), 3.64-3.95 (m, 38H), 3.49-3.52 (m, 4H), 2.21 (s, 6H). The ^{13}C NMR spectrum of **H** is shown in Figure S2. ^{13}C NMR (75 MHz, DMSO-d_6) δ (ppm): 155.4, 150.0, 149.9, 149.8, 149.2, 137.9, 129.8, 129.1, 127.9, 127.6, 127.5, 127.5, 117.7, 114.4, 113.6, 113.3, 67.7, 55.5, 55.4, 29.0, 28.8, 20.3. LRESIMS (m/z): 1075.45 $[M + H]^+$, 1097.45 $[M + Na]^+$. HRESIMS (m/z): calcd for $[M + Na]^+$ $C_{63}H_{70}N_4O_{12}Na$, 1097.4888; found 1097.4904.

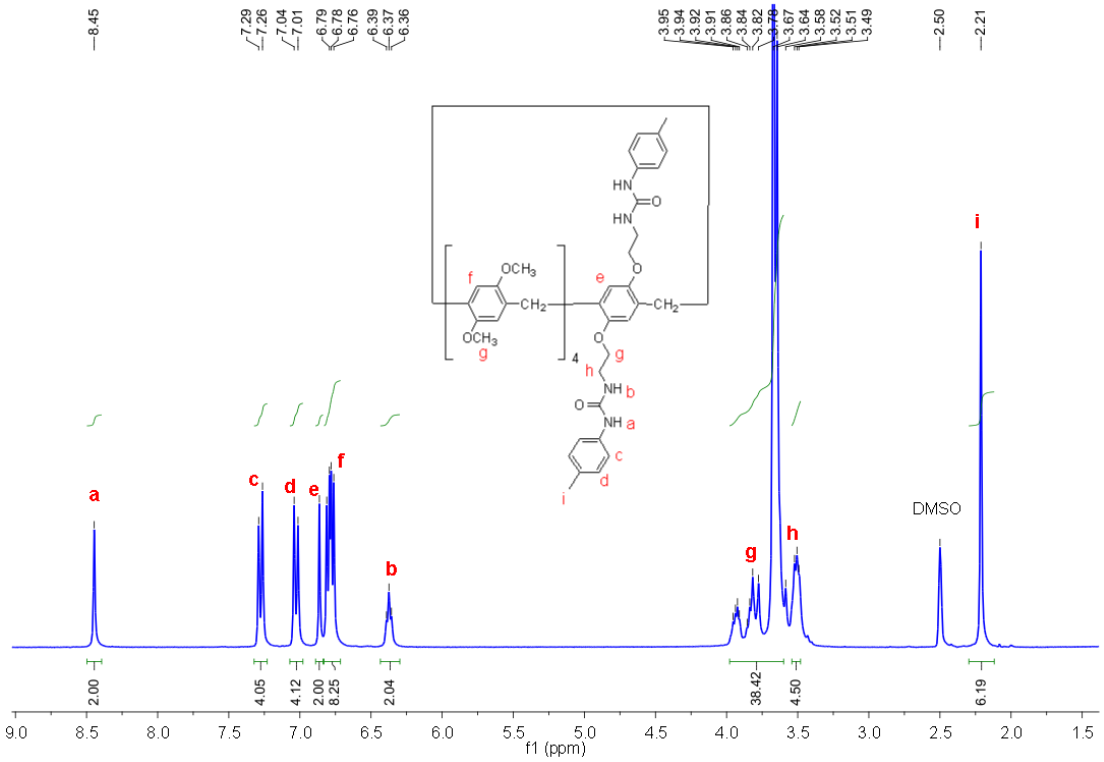

Figure S1. ^{1}H NMR spectrum (300 MHz) of **H** in DMSO-d_6.

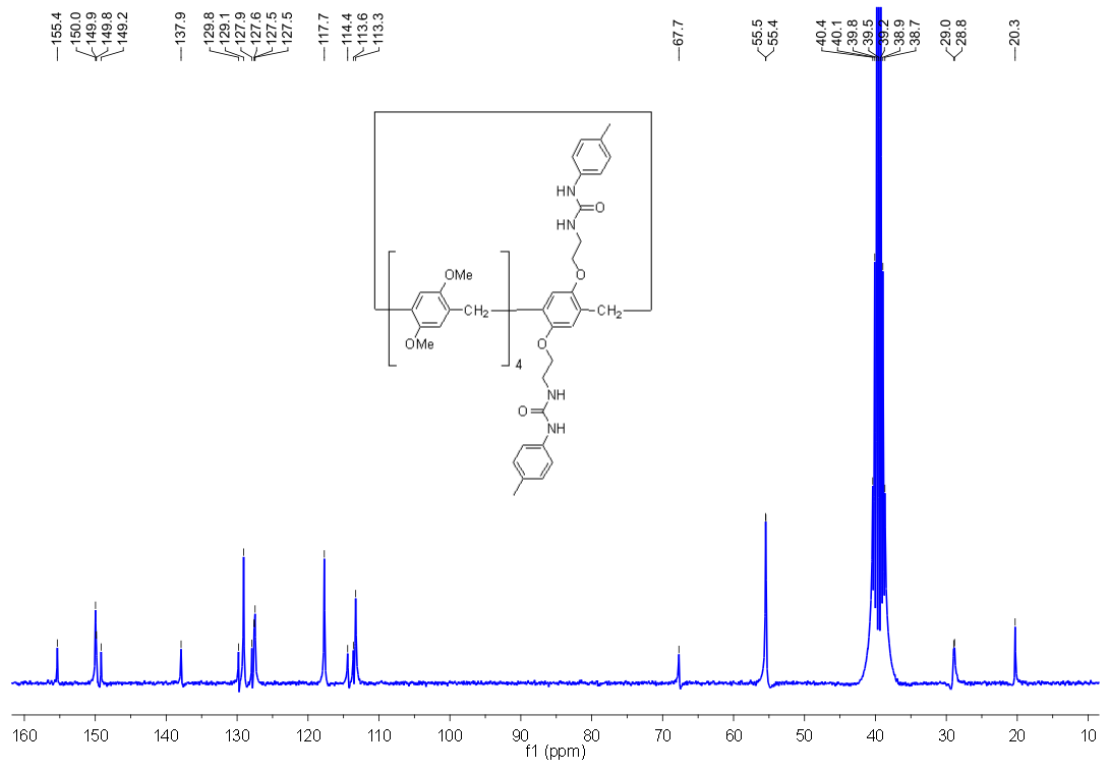

Figure S2. ^{13}C NMR spectrum (75 MHz) of **H** in DMSO-d_6.

*3. General procedure for the synthesis of bis-tetrabutylammonium (TBA) salts of liner alkyl dicarboxylates [**Gn**].*

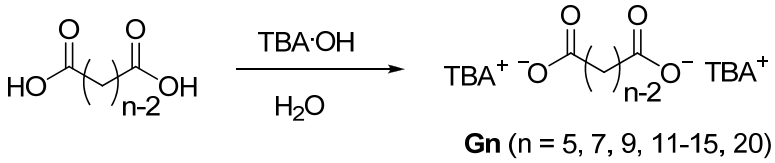

Gn (n = 5, 7, 9, 11-15, 20)

In a typical synthesis tetrabutylammonium hydroxide (10% in water) was added dropwise to a stirred solution of the appropriate diacid (2.0 mmol) in water (10 mL) until the pH = 8. Removal of the solvent by evaporation, compound **Gn** was obtained as a clear paste in good yields (94-99%).

G7 (n =7):

The ^{1}H NMR spectrum of **G7** is shown in Figure S3. ^{1}H NMR (400 MHz, DMSO-d_6) δ (ppm): 3.15-3.19 (m, 16H), 1.66-1.70 (m, 4H), 1.53-1.61 (m, 16H), 1.26-1.35 (m, 20H), 1.03-1.10 (m, 2H), 0.93 (t, J = 7.3 Hz, 24H). The ^{13}C NMR spectrum of **G7** is shown in Figure S4. ^{13}C NMR (100 MHz, DMSO-d_6) δ (ppm): 174.8, 57.5, 39.8, 30.6, 27.3, 23.1, 19.2, 13.5. LRESIMS (m/z): 400.20 [M - TBA]$^-$, 159.00 [M +H - 2TBA]$^-$.

G9 (n = 9):

The ^{1}H NMR spectrum of **G9** is shown in Figure S5. ^{1}H NMR (400 MHz, DMSO-d_6) δ (ppm): 3.15-3.20 (m, 16H), 1.70-1.74 (m, 4H), 1.53-1.61 (m, 16H), 1.27-1.37 (m, 20H), 1.11-1.16 (m, 6H), 0.94 (t, J = 7.3 Hz, 24H). The ^{13}C NMR spectrum of **G9** is shown in Figure S6. ^{13}C NMR (100 MHz, DMSO-d_6) δ (ppm): 174.7, 57.5, 29.9, 29.6, 27.0, 23.1, 19.2, 13.5. LRESIMS (m/z): 428.25 [M - TBA]$^-$, 187.00 [M +H - 2TBA]$^-$.

G11 (n = 11):

The ^{1}H NMR spectrum of **G11** is shown in Figure S7. ^{1}H NMR (400 MHz, DMSO-d_6) δ (ppm): 3.16-3.20 (m, 16H), 1.71-1.75 (m, 4H), 1.53-1.61 (m, 16H), 1.27-1.36 (m, 20H), 1.14-1.19 (m, 10H), 0.94 (t, J = 7.3 Hz, 24H). The ^{13}C NMR spectrum of **G11** is shown in Figure S8. ^{13}C NMR (100 MHz, DMSO-d_6) δ (ppm): 174.8, 57.5, 39.4, 29.8, 29.4, 29.4, 26.9, 23.1, 19.2, 13.5. LRESIMS (m/z): 456.25 [M - TBA]$^-$, 215.05 [M +H - 2TBA]$^-$.

G12 (n = 12):

The ^{1}H NMR spectrum of **G12** is shown in Figure S9. ^{1}H NMR (300 MHz, DMSO-d_6) δ (ppm): 3.15-3.20 (m, 16H), 1.71 (t, J = 7.4 Hz, 4H), 1.52-1.62 (m, 16H), 1.24-1.36 (m, 20H), 1.11-1.19 (m, 12H), 0.93 (t, J = 7.3 Hz, 24H). The ^{13}C NMR spectrum of **G12** is shown in Figure S10. ^{13}C NMR (100 MHz, DMSO-d_6) δ (ppm): 174.6, 57.5, 39.4, 29.8, 29.4, 29.3, 26.9, 23.1, 19.2, 13.5. LRESIMS (m/z): 470.30 [M - TBA]$^-$, 229.05 [M +H - 2TBA]$^-$.

G13 (n = 13):

The ^{1}H NMR spectrum of **G13** is shown in Figure S11. ^{1}H NMR (300 MHz, DMSO-d_6) δ (ppm): 3.17-3.22 (m, 16H), 1.77 (t, J = 7.4 Hz, 4H), 1.53-1.63 (m, 16H), 1.21-1.41 (m, 34H), 0.93 (t, J = 7.3 Hz, 24H). The ^{13}C NMR spectrum of **G13** is shown in Figure S12. ^{13}C NMR (75 MHz, DMSO-d_6) δ (ppm): 174.9, 57.5, 38.9, 29.60, 29.3, 29.2, 26.7, 23.1, 19.2, 13.5. LRESIMS (m/z): 484.40 [M - TBA]$^-$, 243.10 [M +H - 2TBA]$^-$.

G14 (n = 14):

The ^{1}H NMR spectrum of **G14** is shown in Figure S13. ^{1}H NMR (400 MHz, DMSO-d_6) δ (ppm): 3.16-3.20 (m, 16H), 1.74 (t, J = 7.4 Hz, 4H), 1.53-1.61 (m, 16H), 1.27-1.39 (m, 20H), 1.19-1.22 (m, 16H), 0.94 (t, J = 7.3 Hz, 24H). The ^{13}C NMR spectrum of **G14** is shown in Figure S14. ^{13}C NMR (100 MHz, DMSO-d_6) δ (ppm): 174.8, 57.5, 29.6, 29.3, 29.2, 29.2, 26.8, 23.1, 19.2, 13.5. LRESIMS (m/z): 498.30 [M - TBA]$^-$, 257.05 [M +H - 2TBA]$^-$.

G15 (n = 15):

The ^{1}H NMR spectrum of **G15** is shown in Figure S15. ^{1}H NMR (400 MHz, DMSO-d_6) δ (ppm): 3.16-3.20 (m, 16H), 1.73 (t, J = 7.4 Hz, 4H), 1.53-1.61 (m, 16H), 1.26-1.38 (m, 20H), 1.14-1.22 (m, 18H), 0.94 (t, J = 7.3 Hz, 24H). The ^{13}C NMR spectrum of **G15** is shown in Figure S16. ^{13}C NMR (100 MHz, DMSO-d_6) δ (ppm): 174.7, 57.5, 39.2, 29.7, 29.3, 29.2, 29.2, 26.8, 23.1, 19.2, 13.5. LRESIMS (m/z): 512.30 [M - TBA]$^-$, 271.05 [M +H - 2TBA]$^-$.

G20 (n = 20):

The ^{1}H NMR spectrum of **G20** is shown in Figure S17. ^{1}H NMR (400 MHz, DMSO-d_6) δ (ppm): 3.15-3.19 (m, 16H), 1.75 (t, J = 7.4 Hz, 4H), 1.55 (m, 16H), 1.31 (m, 48H), 0.94 (t, J = 7.3 Hz, 24H). The ^{13}C NMR spectrum of **G20** is shown in Figure S18. ^{13}C NMR (100 MHz, DMSO-d_6) δ (ppm): 175.2, 57.6, 39.2, 29.7, 29.3, 29.2, 29.2, 29.1, 29.1, 26.8, 23.1, 19.2, 13.5. LRESIMS (m/z): 582.35 [M - TBA]$^-$, 341.15 [M +H - 2TBA]$^-$.

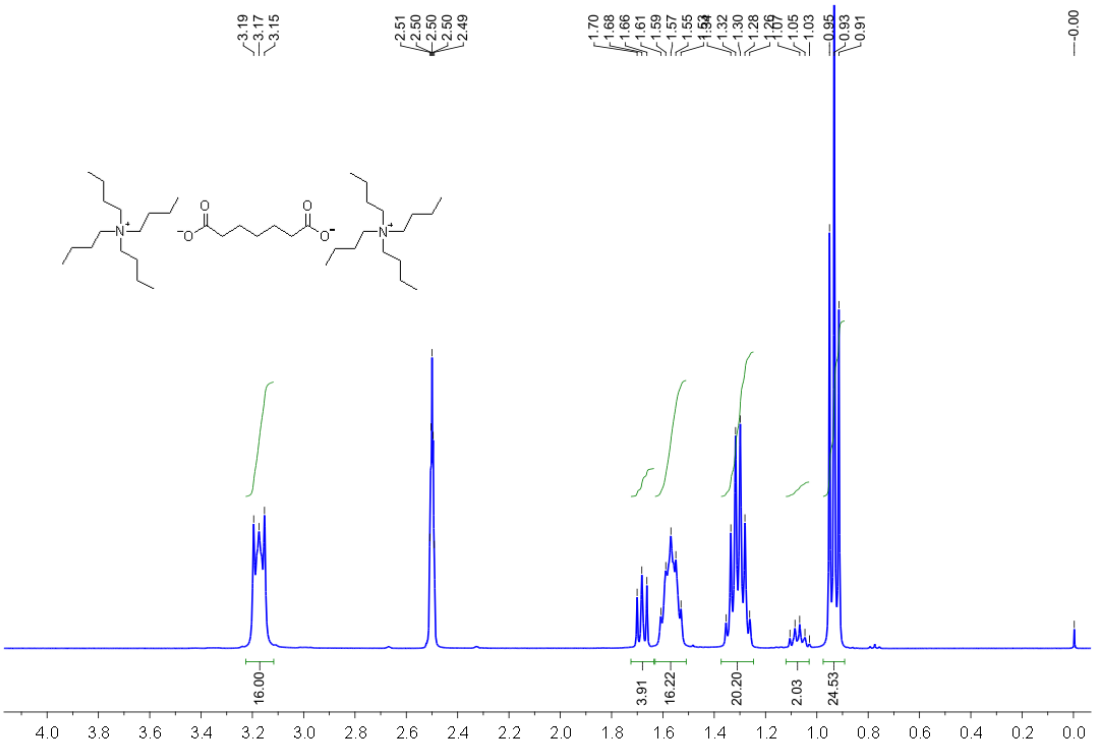

Figure S3. ^{1}H NMR spectrum (400 MHz) of **G7** in DMSO-d_6.

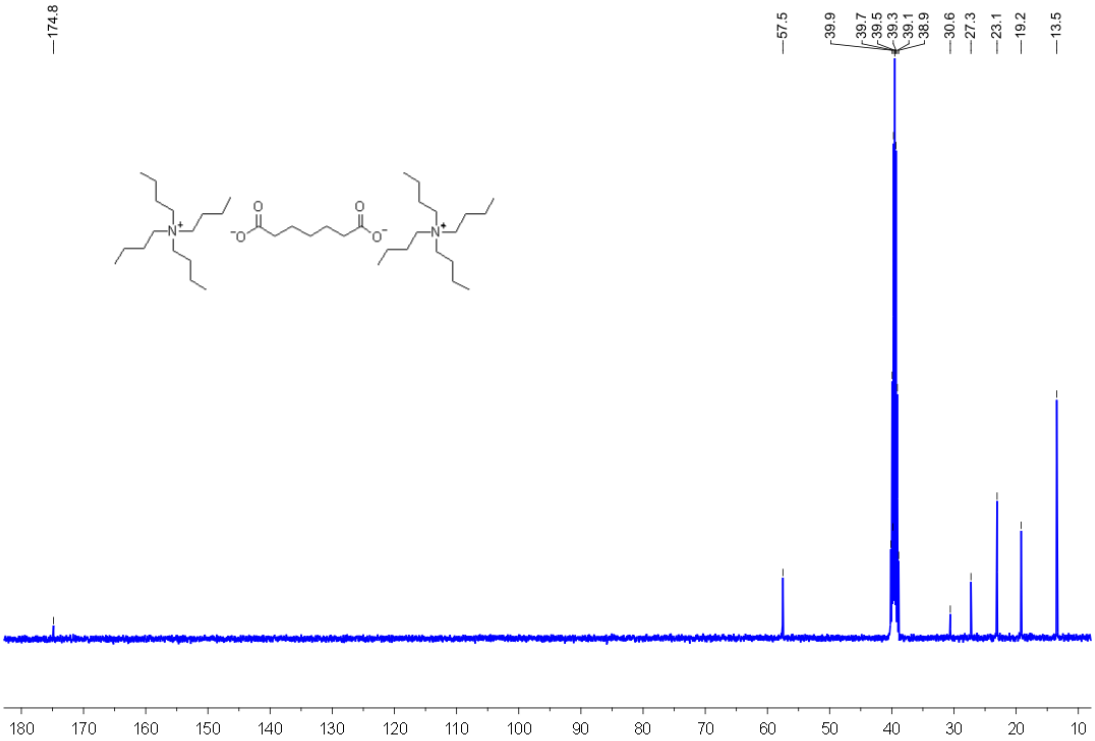

Figure S4. ^{13}C NMR spectrum (100 MHz) of **G7** in DMSO-d_6.

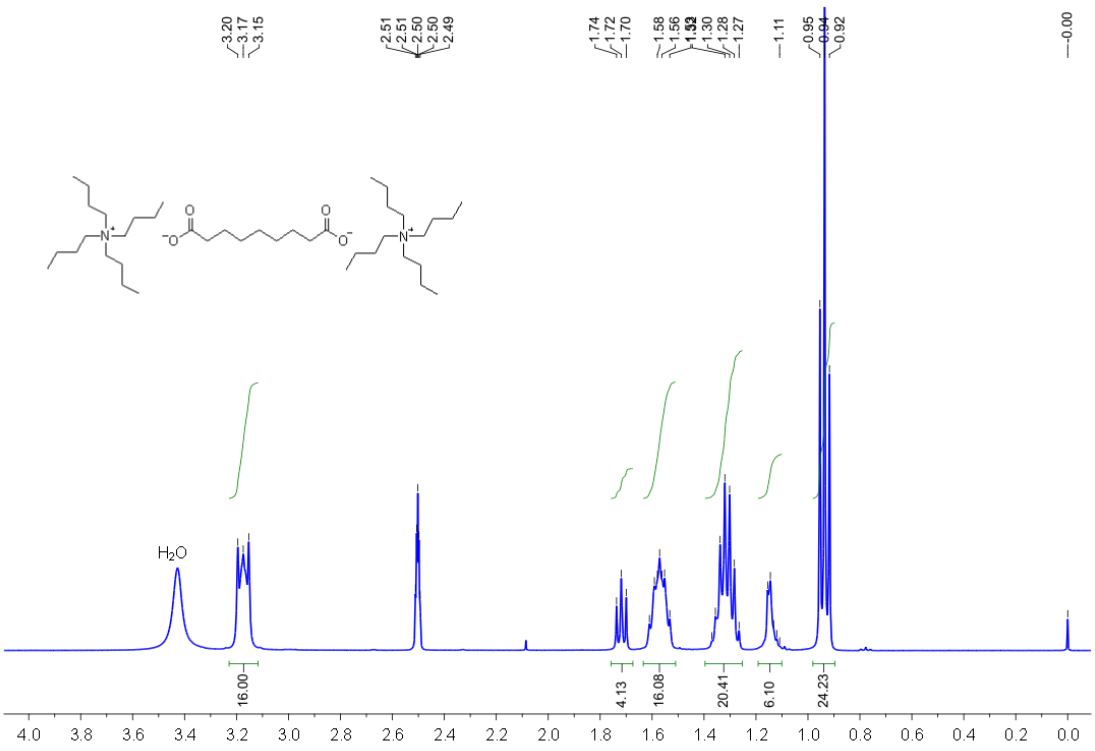

Figure S5. ^{1}H NMR spectrum (400 MHz) of **G9** in DMSO-d_6.

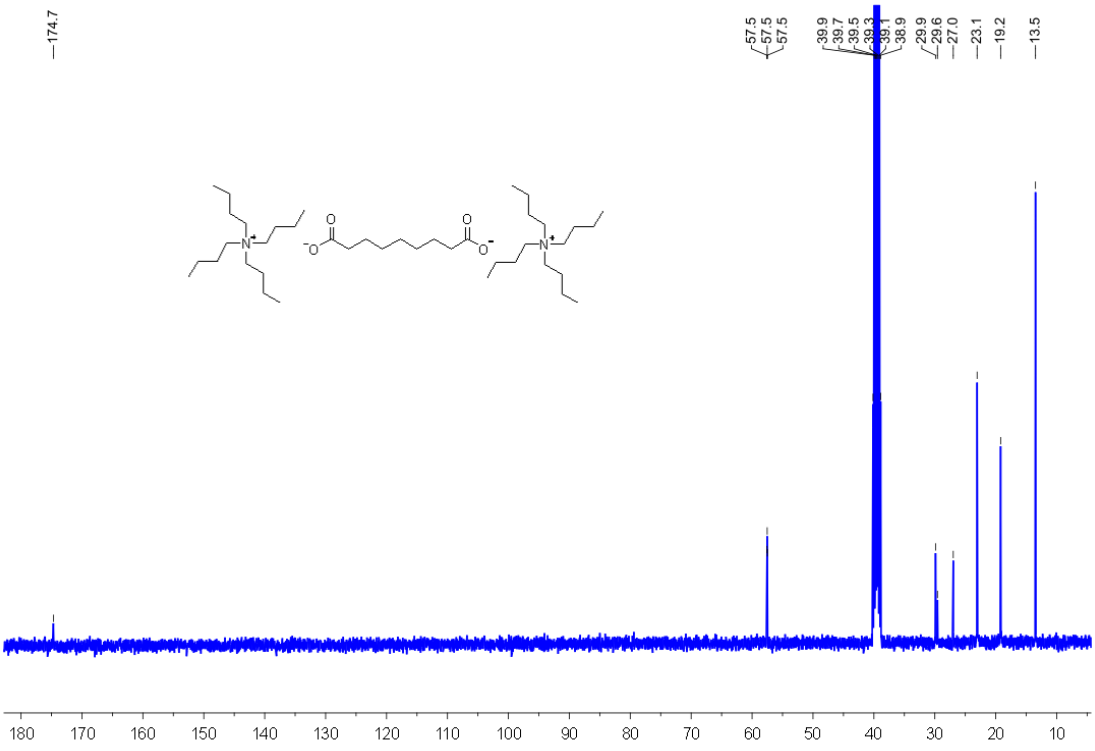

Figure S6. ^{13}C NMR spectrum (100 MHz) of **G9** in DMSO-d_6.

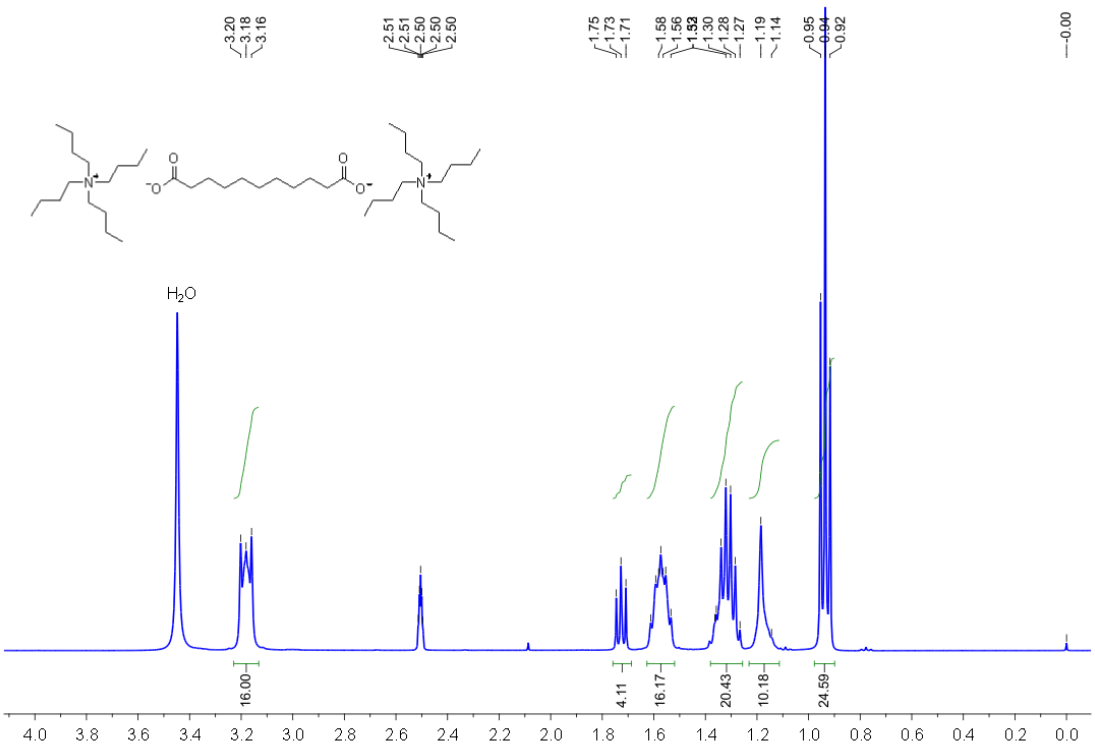

Figure S7. ^{1}H NMR spectrum (400 MHz) of **G11** in DMSO-d_6.

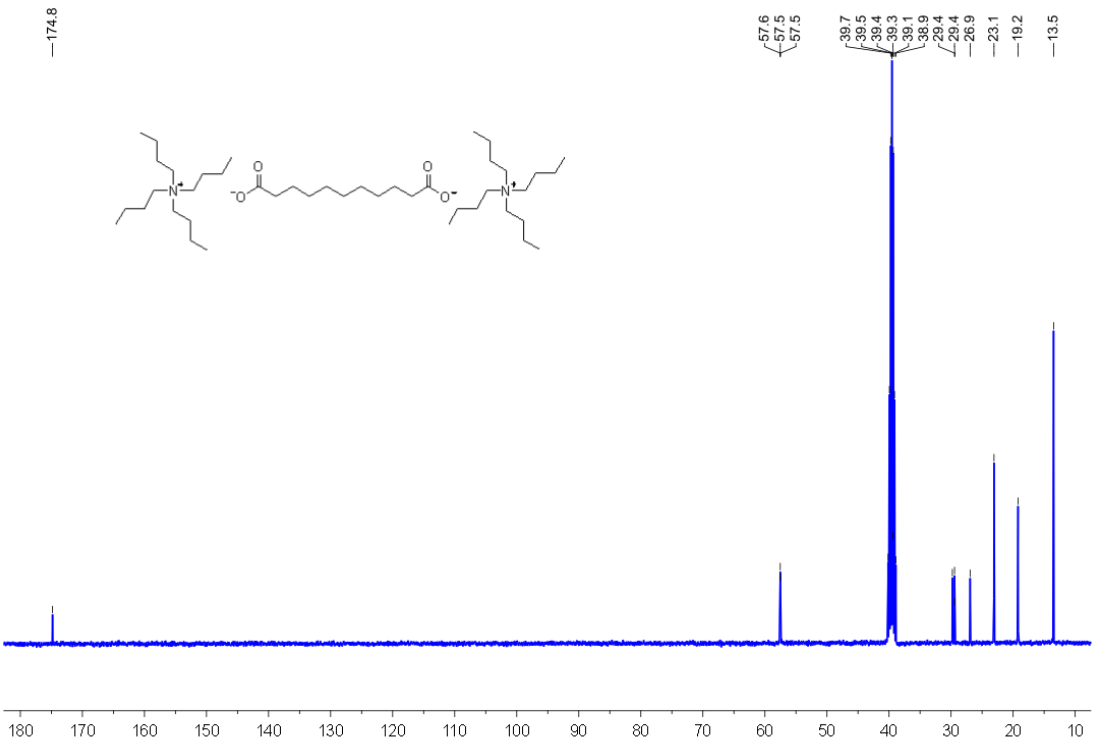

Figure S8. ^{13}C NMR spectrum (100 MHz) of **G11** in DMSO-d_6.

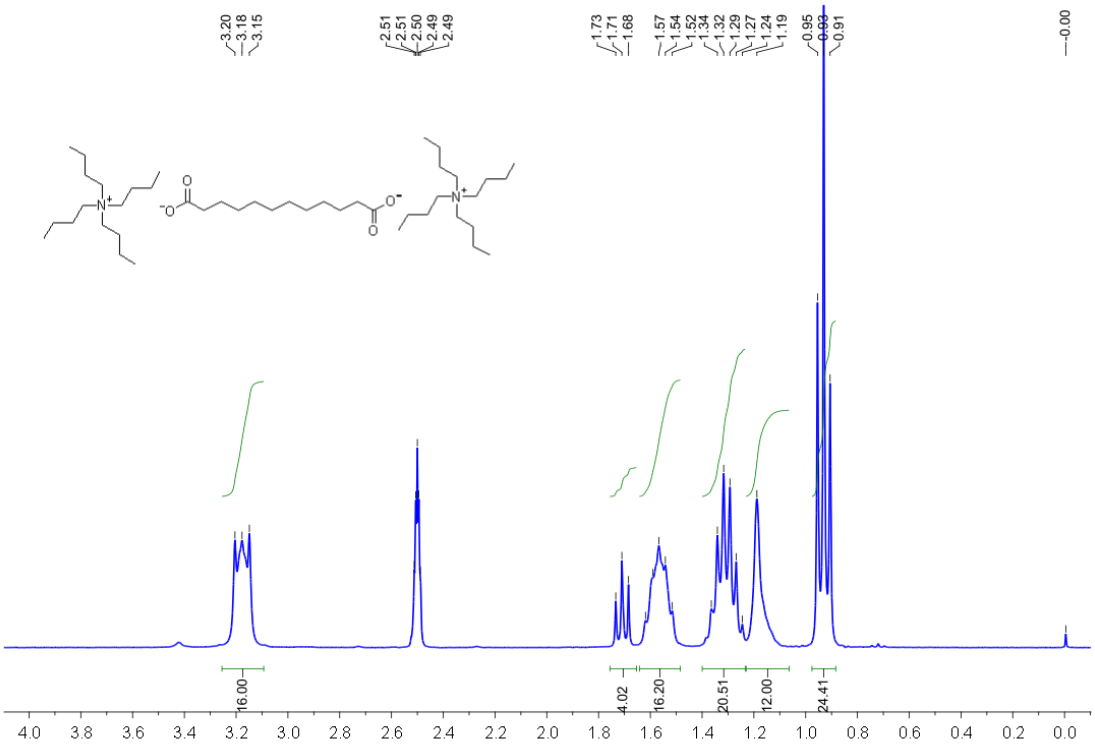

Figure S9. ^{1}H NMR spectrum (300 MHz) of **G12** in DMSO-d_6.

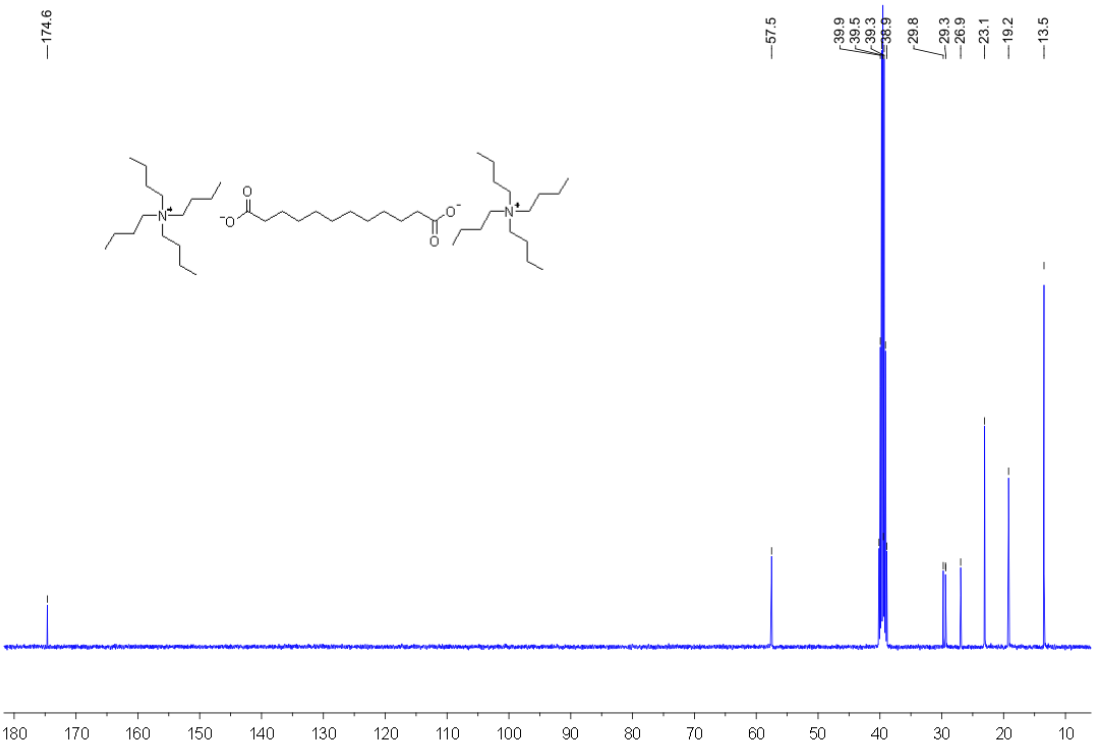

Figure S10. ^{13}C NMR spectrum (100 MHz) of **G12** in DMSO-d_6.

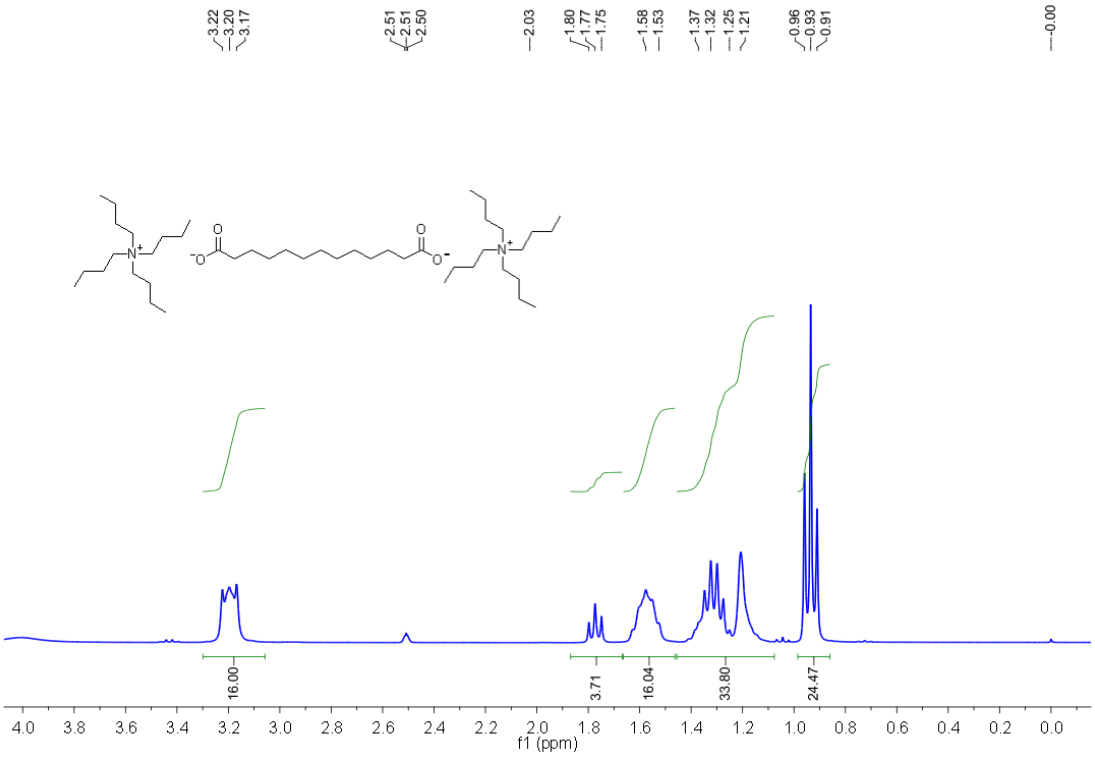

Figure S11. ^{1}H NMR spectrum (300 MHz) of **G13** in DMSO-d_6.

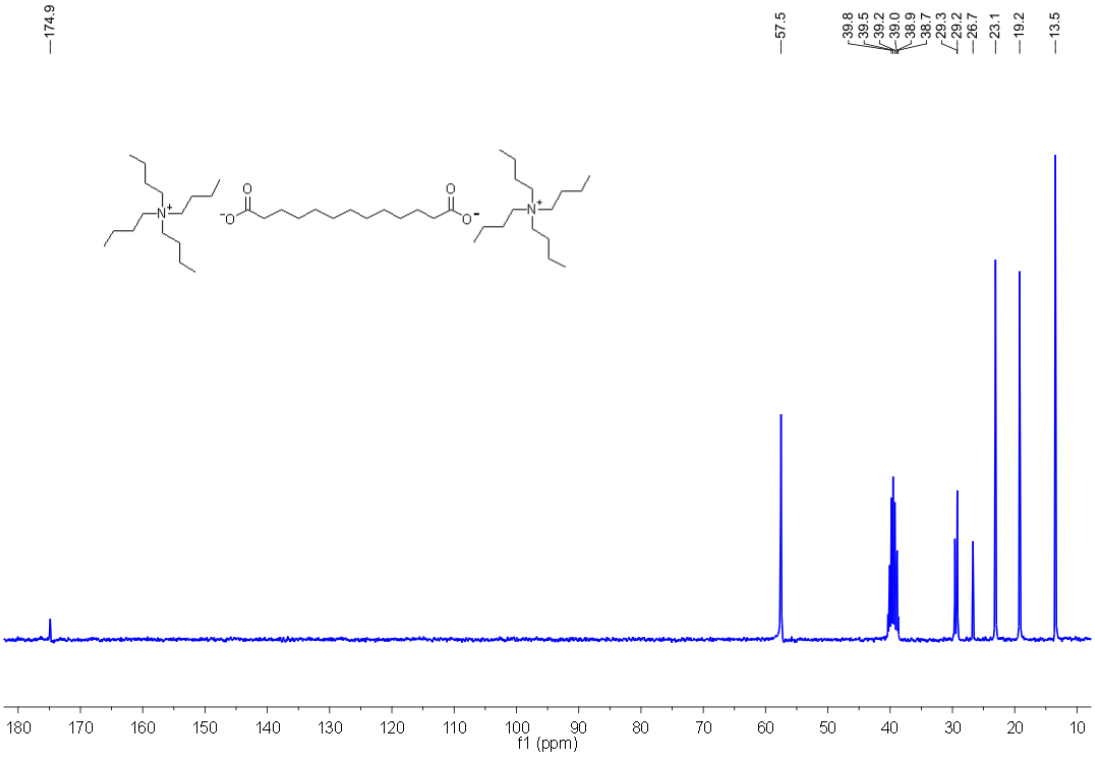

Figure S12. ^{13}C NMR spectrum (75 MHz) of **G13** in DMSO-d_6.

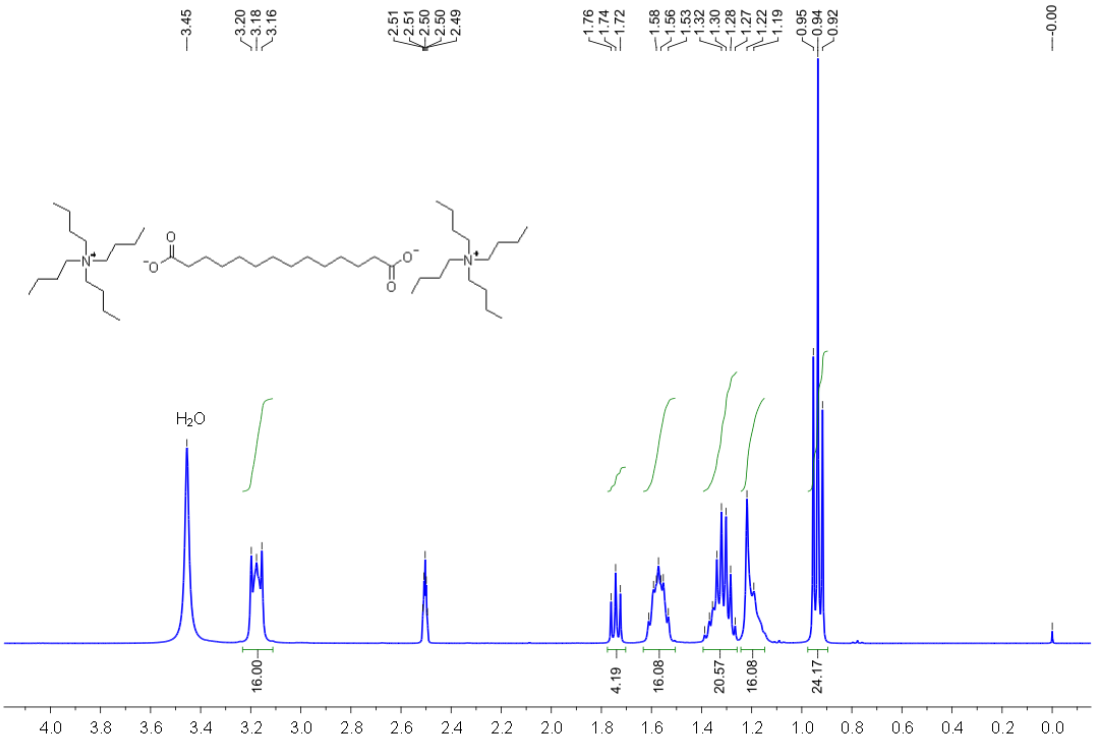

Figure S13. ^{1}H NMR spectrum (400 MHz) of **G14** in DMSO-d_6.

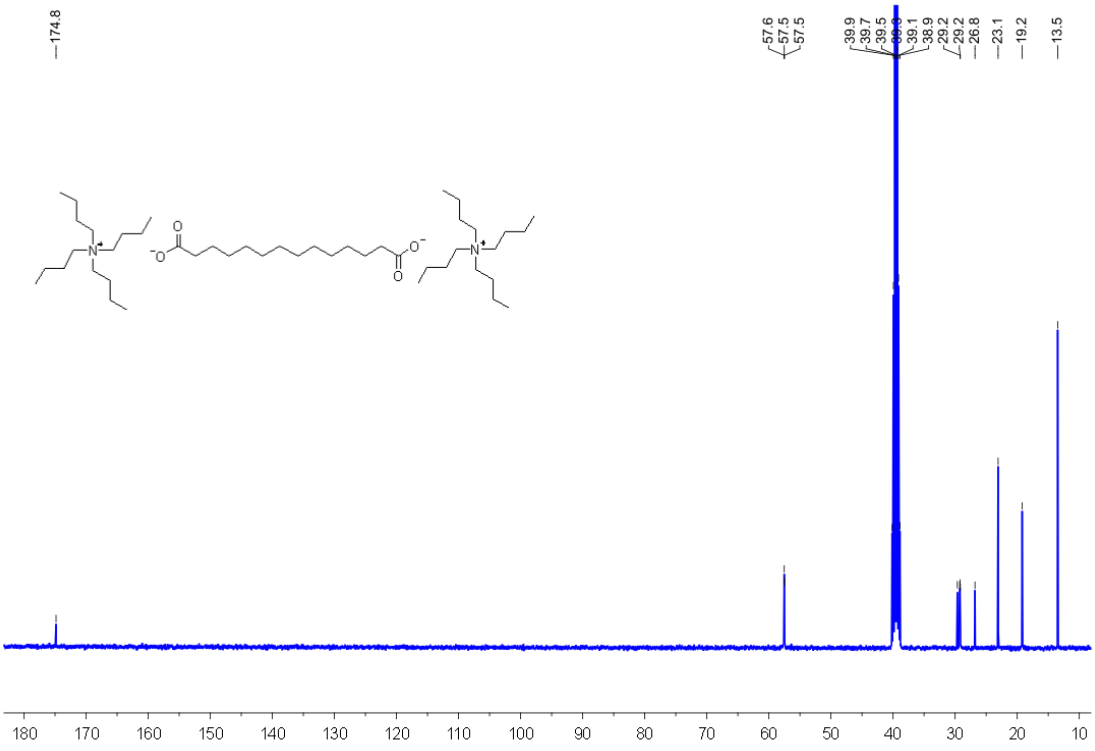

Figure S14. ^{13}C NMR spectrum (100 MHz) of **G14** in DMSO-d_6.

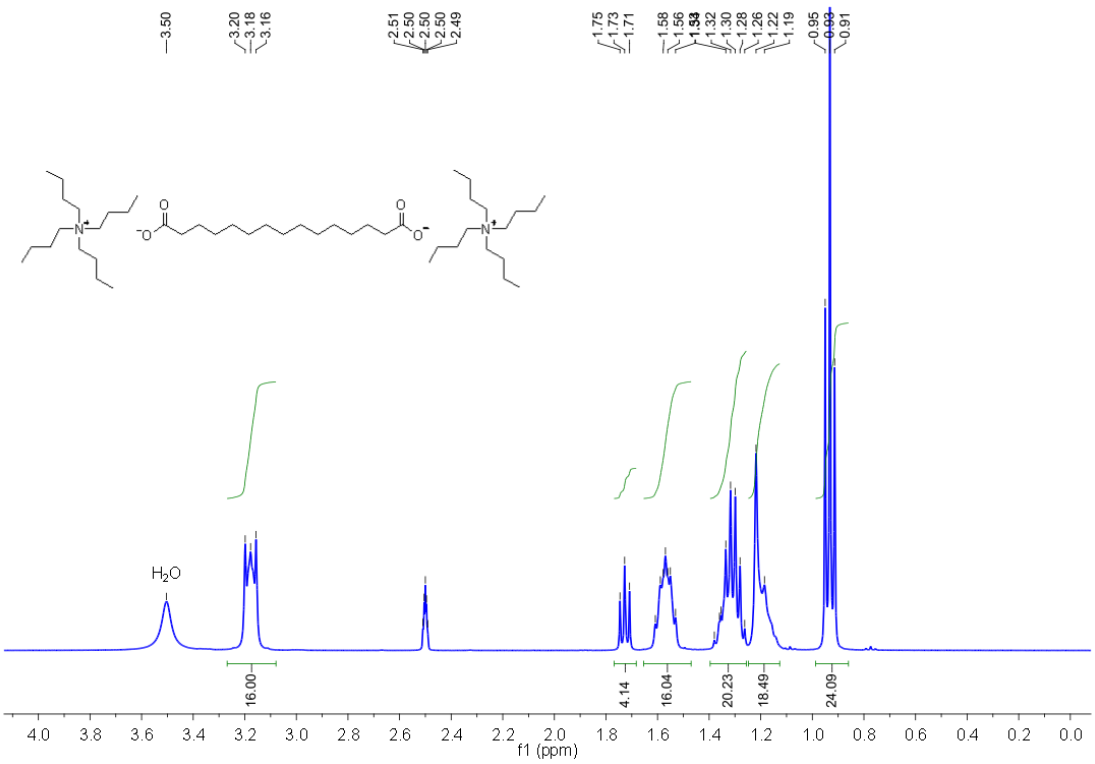

Figure S15. ^{1}H NMR spectrum (400 MHz) of **G15** in DMSO-d_6.

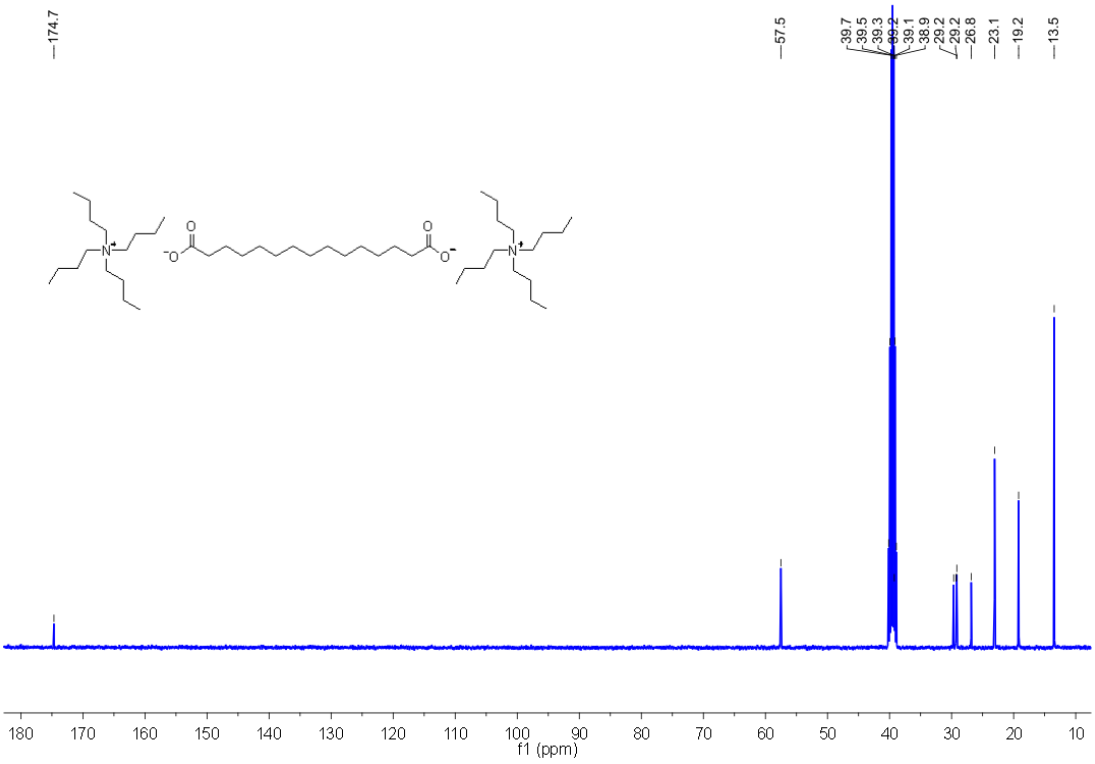

Figure S16. ^{13}C NMR spectrum (100 MHz) of **G15** in DMSO-d_6.

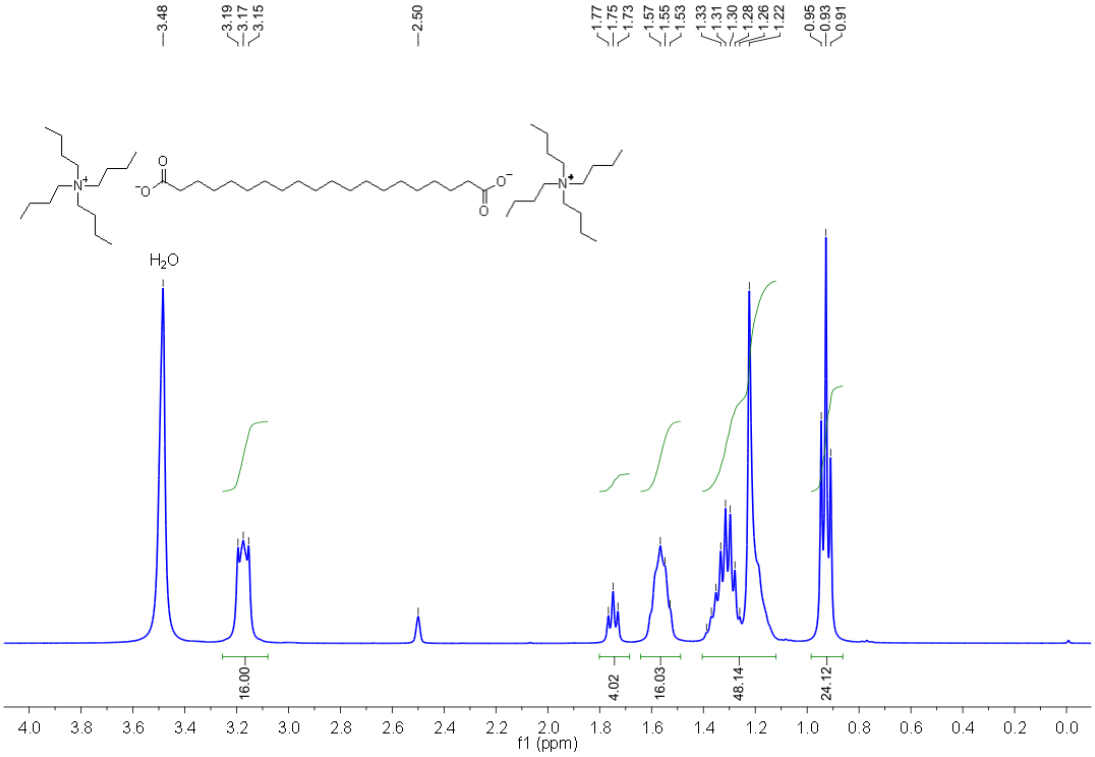

Figure S17. ^{1}H NMR spectrum (400 MHz) of **G20** in DMSO-d_6.

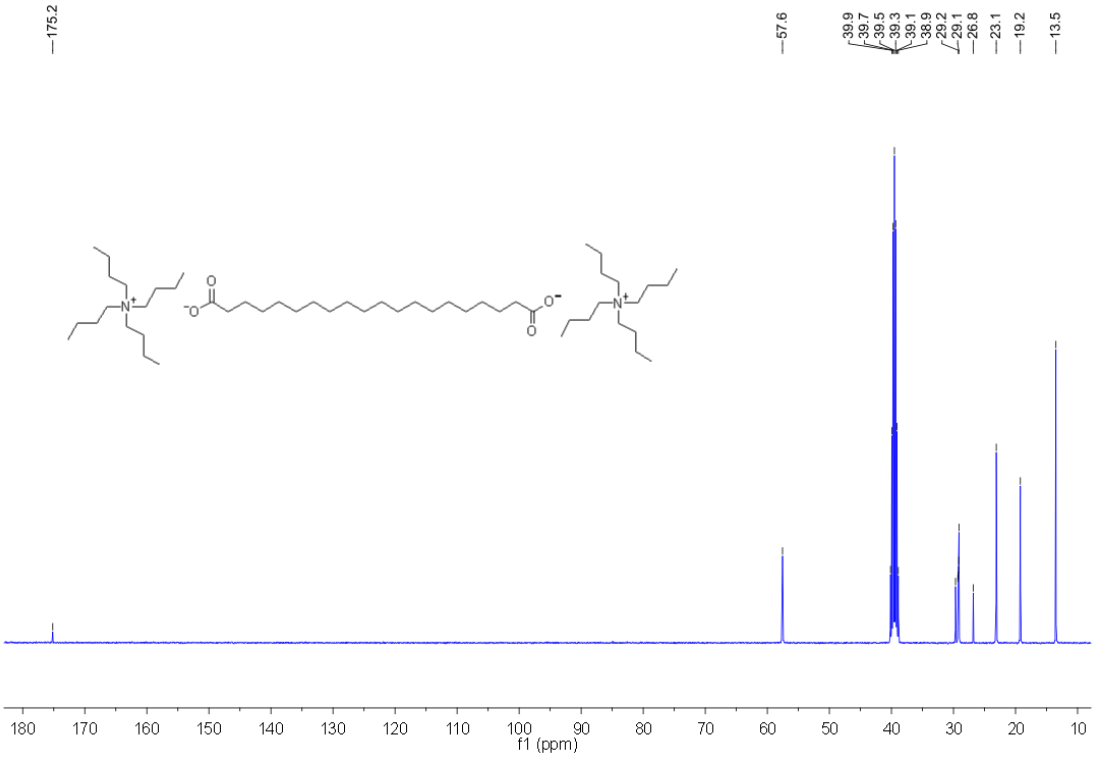

Figure S18. ^{13}C NMR spectrum (100 MHz) of **G20** in DMSO-d_6.

4. 2D NOESY analysis of ***G13*** *with* ***H****.*

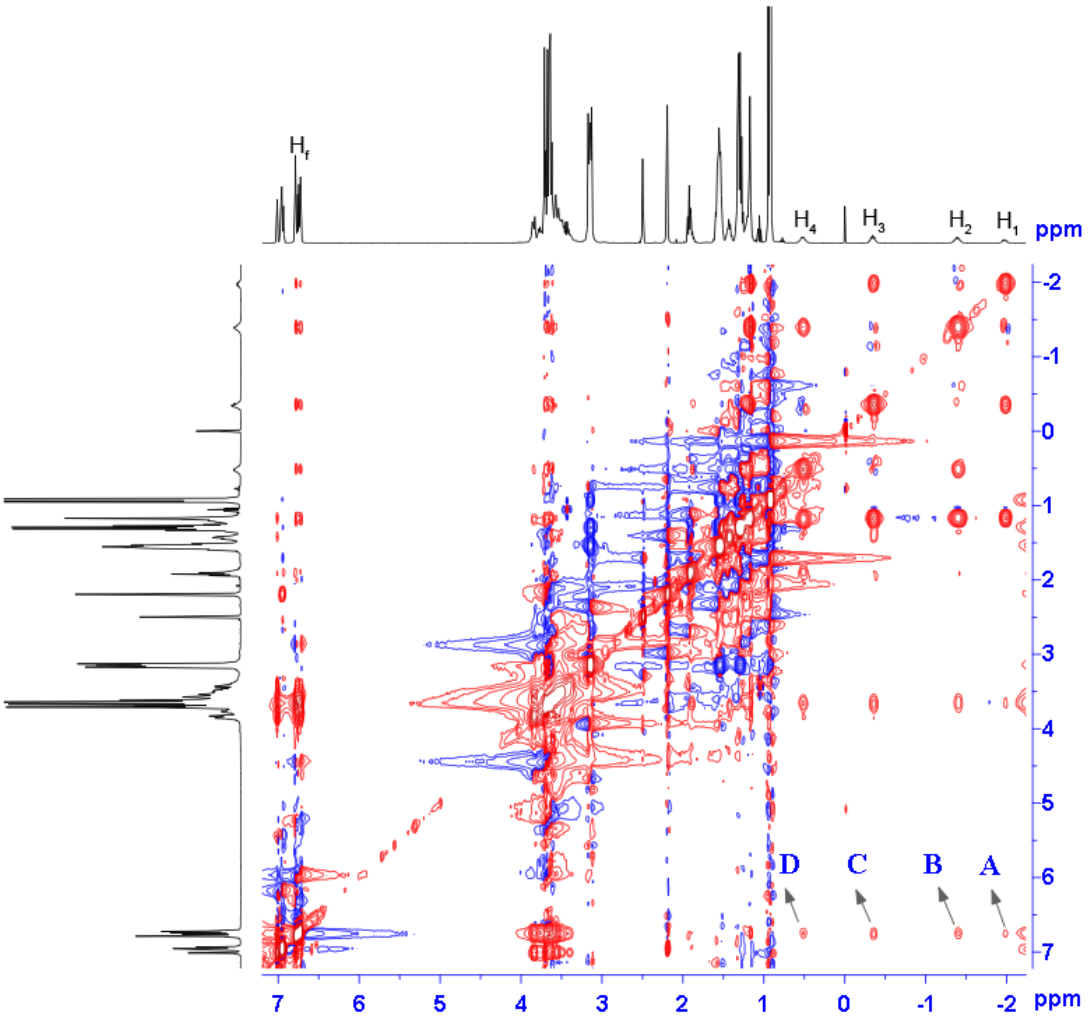

Figure S19. 2D NOESY analysis of **G13** (30 mM) with **H** (20 mM) in DMSO-d_6 (400 MHz, 298 K) with a mixing time of 300 ms. NOE correlations (marked with A,B,C and D) were observed between methylene protons of **G13** and aromatic protons of **H**, indicating that **G13** threaded within the cavity of **H**.

5. Job plot for ***G13*** ⊂ ***H***

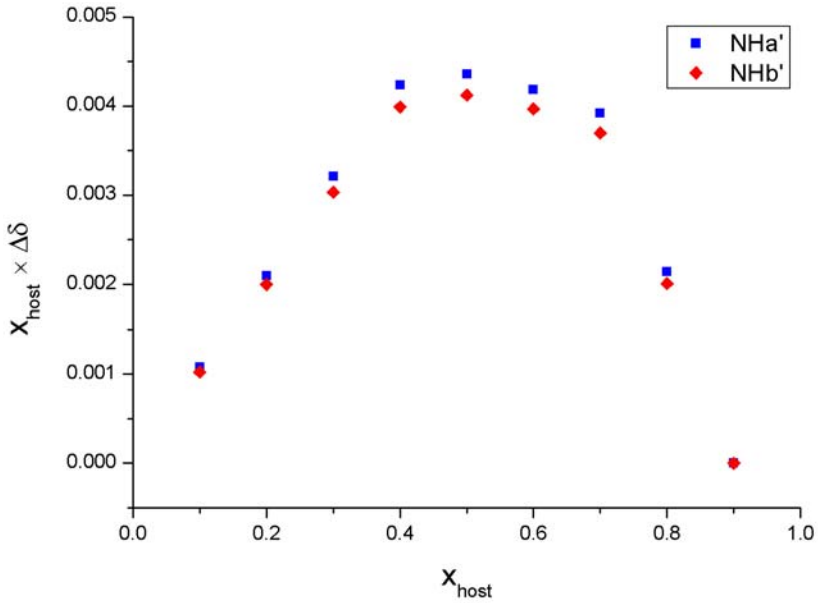

Figure S20. Job plot between bis-urea-functionalized pillar[5]arene **H** (host) and bis-TBA salt of tridecanedioate **G13** collected by plotting the Δδ in chemical shift of the urea protons $H_{a'}$ and $H_{b'}$ from interpenetrated **H** observed by ^{1}H NMR spectroscopy (DMSO-d_6) against the change in the mole fraction of the host (X_{host}). The plot indicates a 1:1 binding ratio between the host and guest.

6. Schematic representation of external complicated complexes of ***H*** *and* ***Gn***

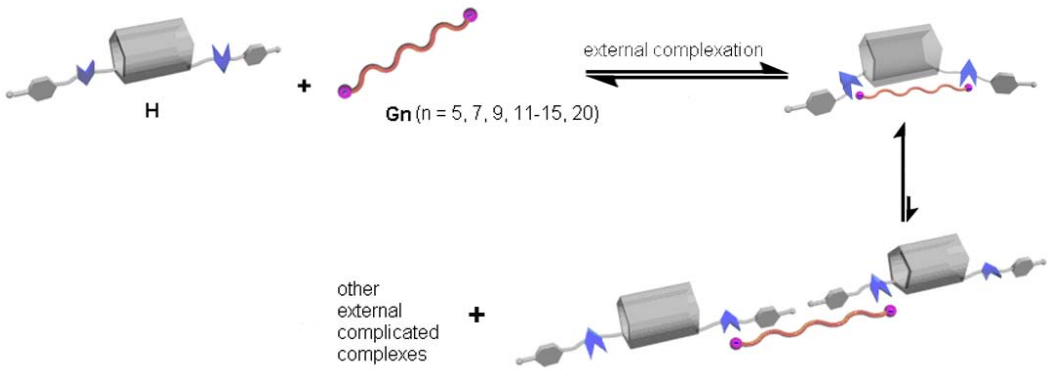

Scheme S2. Schematic illustration of the formation of external complicated complexes from **H** and **Gn**.

7. *^{1}H NMR spectra of* ***H*** *in the absence and presence of* ***Gn***.

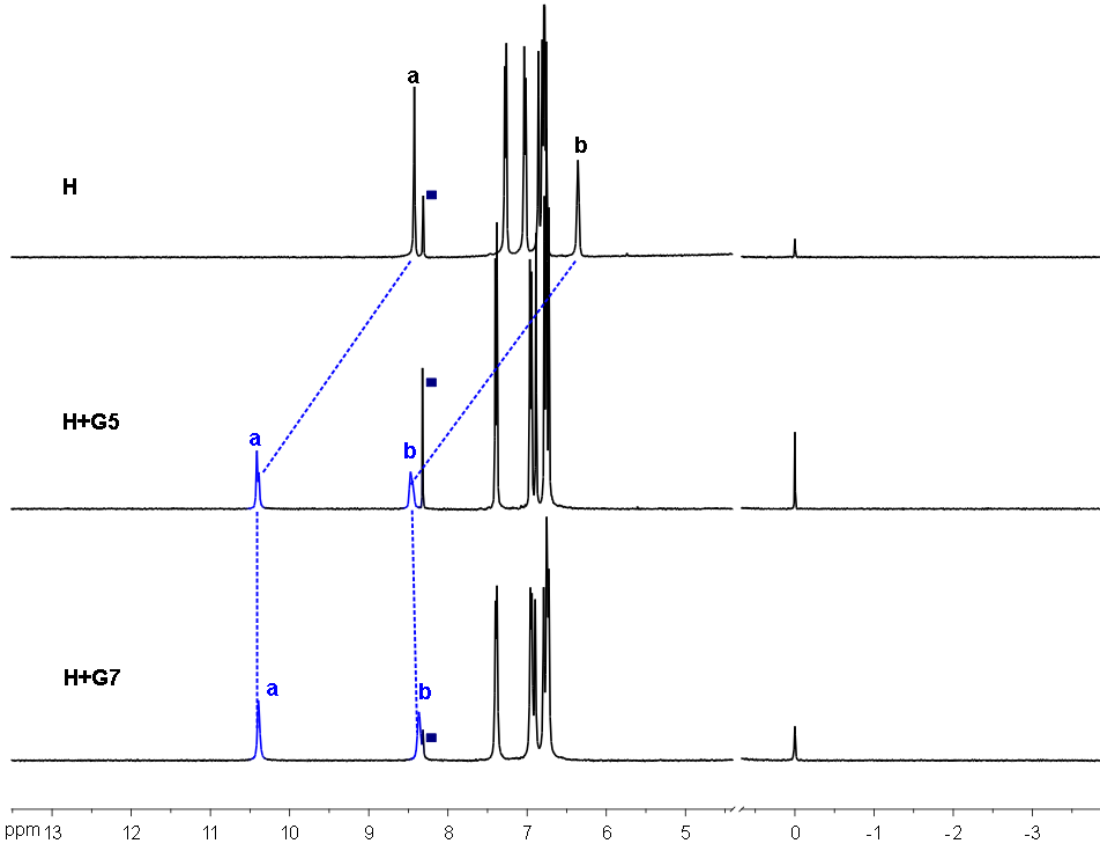

Figure S21. Partial ^{1}H NMR spectra (400 MHz, 298K) of **H** (10 mM) and its mixture with **G5** (10 mM) and **G7** (10 mM) in DMSO-d_6. (**a** and **b**: signals of urea protons on **H**; the peaks marked with ■ are ascribed to chloroform).

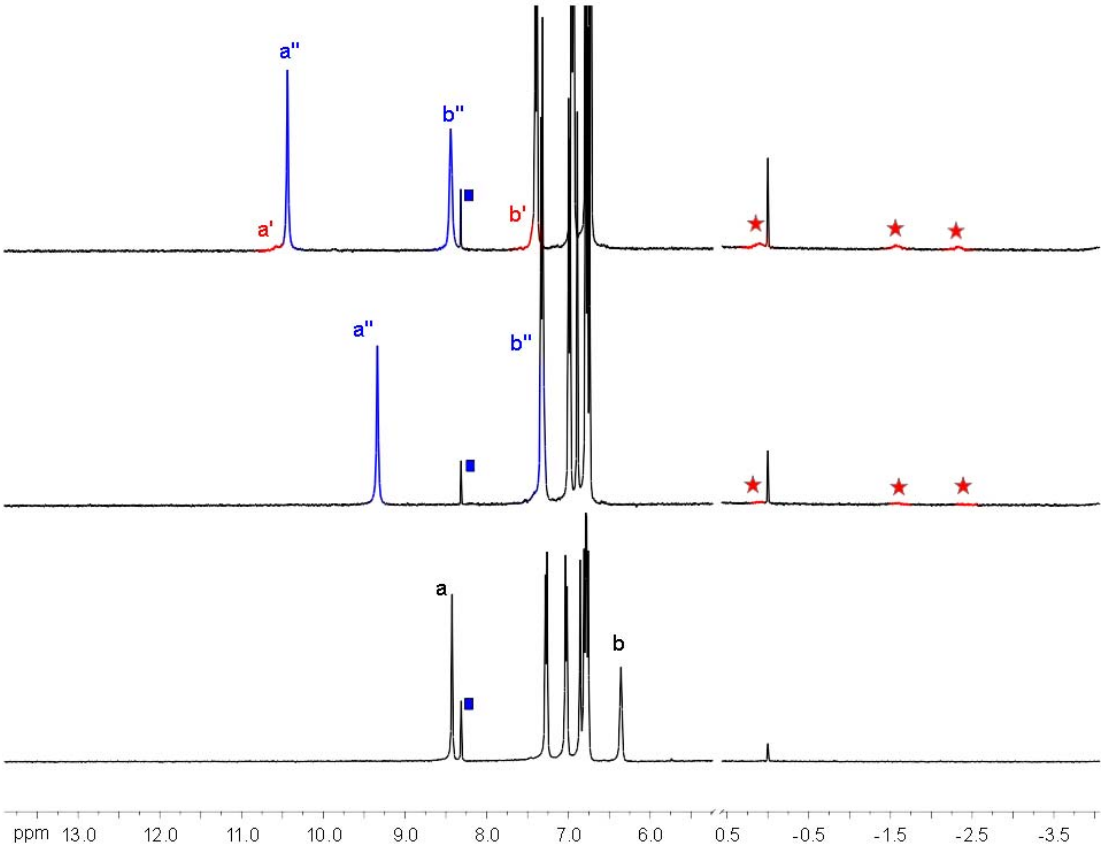

Figure S22. Partial ^{1}H NMR spectra (400 MHz, 298K) of **H** (10 mM) in the presence of increasing amounts of **G9**; from bottom to top: 0.0, 0.8, and 1.5 equivalents. (**a′** and **b′**: signals of urea protons from interpenetrated **H**; **a″** and **b″**: signals of urea protons from non-interpenetrated **H**; ★: signals from methylene protons of encapsulated **G9**; the peaks marked with ■ are ascribed to chloroform).

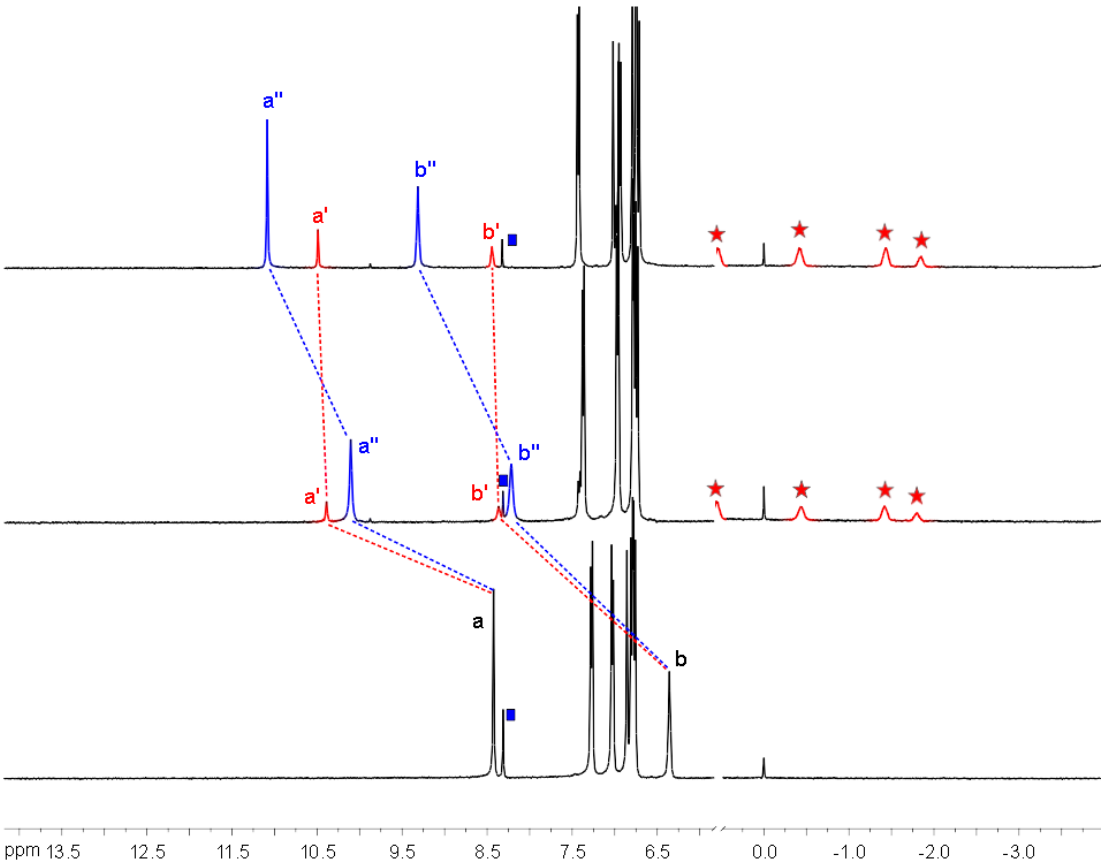

Figure S23. Partial ^{1}H NMR spectra (400 MHz, 298K) of **H** (10 mM) in the presence of increasing amounts of **G11**; from bottom to top: 0.0, 0.8, and 1.5 equivalents. (**a′** and **b′**: signals of urea protons from interpenetrated **H**; **a″** and **b″**: signals of urea protons from non-interpenetrated **H**; ★: signals from methylene protons of encapsulated **G11**; the peaks marked with ■ are ascribed to chloroform).

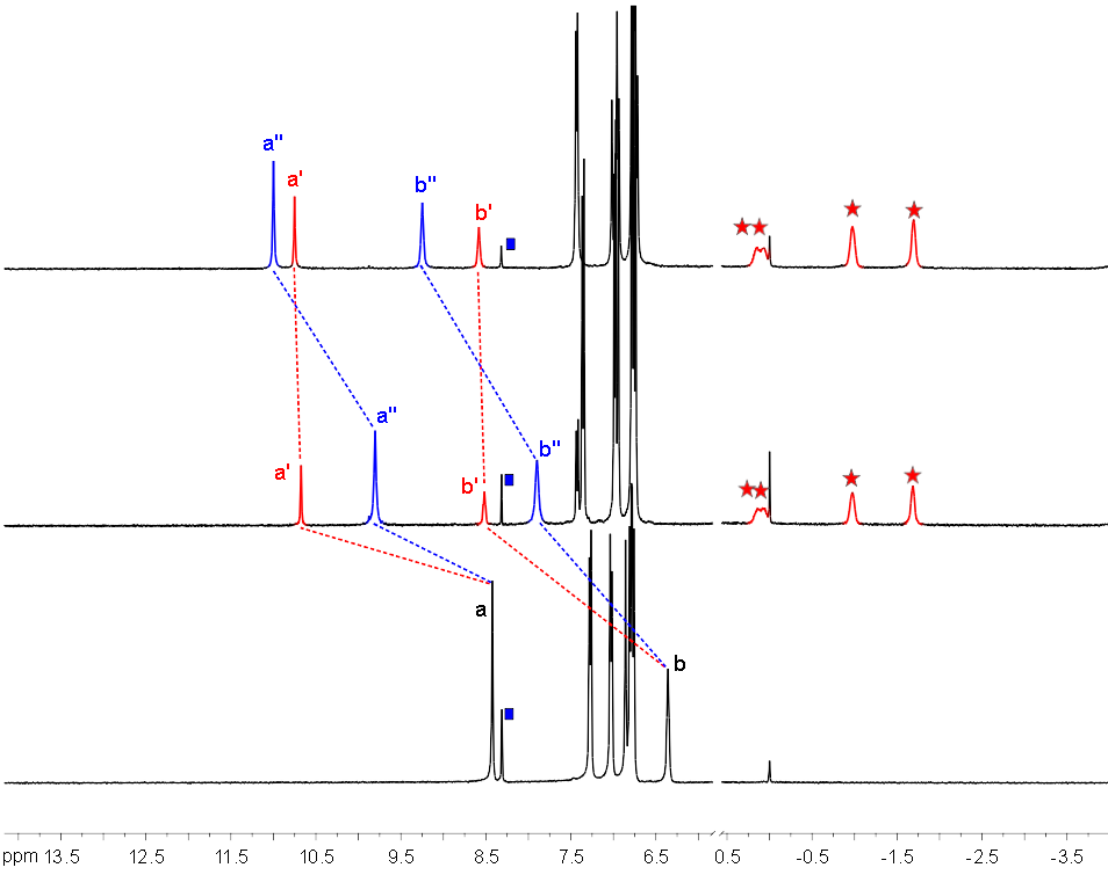

Figure S24. Partial ^{1}H NMR spectra (400 MHz, 298K) of **H** (10 mM) in the presence of increasing amounts of **G12**; from bottom to top: 0.0, 0.8, and 1.5 equivalents. (**a′** and **b′**: signals of urea protons from interpenetrated **H**; **a″** and **b″**: signals of urea protons from non-interpenetrated **H**; ★: signals from methylene protons of encapsulated **G12**; the peaks marked with ■ are ascribed to chloroform).

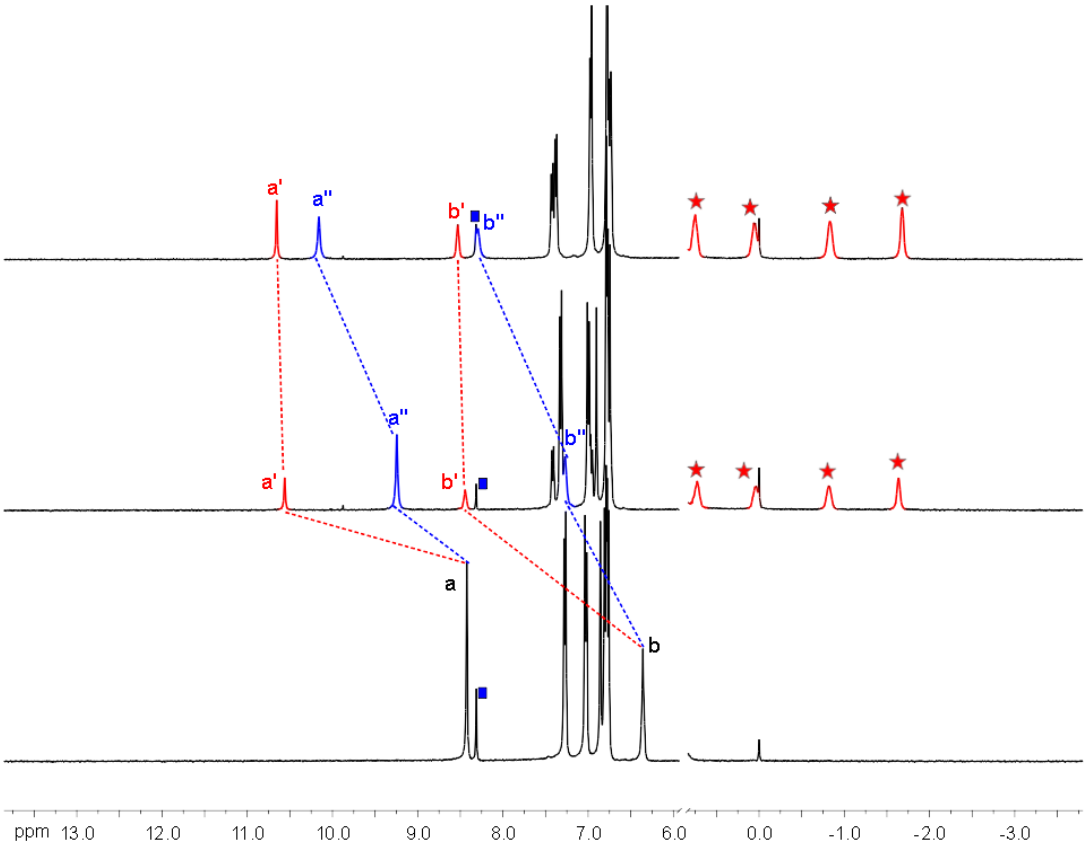

Figure S25. Partial ^{1}H NMR spectra (400 MHz, 298K) of **H** (10 mM) in the presence of increasing amounts of **G14**; from bottom to top: 0.0, 0.8, and 1.5 equivalents. (**a′** and **b′**: signals of urea protons from interpenetrated **H**; **a″** and **b″**: signals of urea protons from non-interpenetrated **H**; ★: signals from methylene protons of encapsulated **G14**; the peaks marked with ■ are ascribed to chloroform).

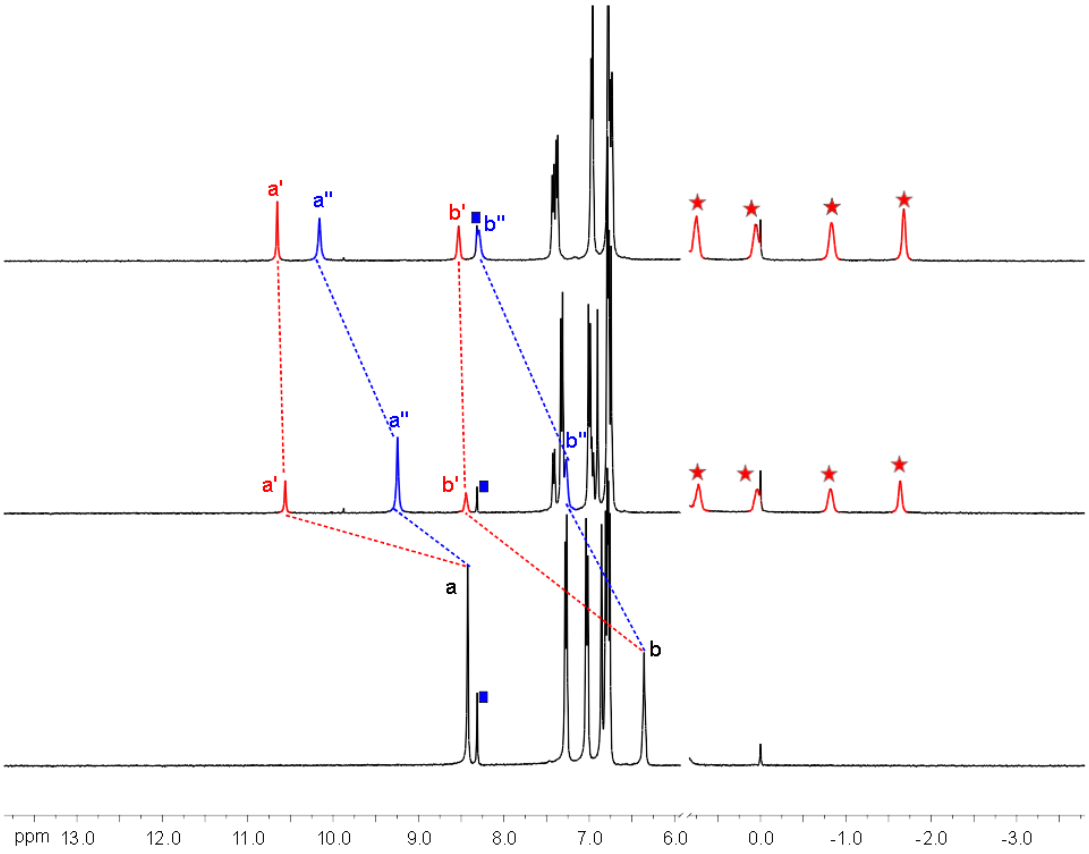

Figure S26. Partial ^{1}H NMR spectra (400 MHz, 298K) of **H** (10 mM) in the presence of increasing amounts of **G15**; from bottom to top: 0.0, 0.8, and 1.5 equivalents. (**a′** and **b′**: signals of urea protons from interpenetrated **H**; **a″** and **b″**: signals of urea protons from non-interpenetrated **H**; ★: signals from methylene protons of encapsulated **G15**; the peaks marked with ■ are ascribed to chloroform).

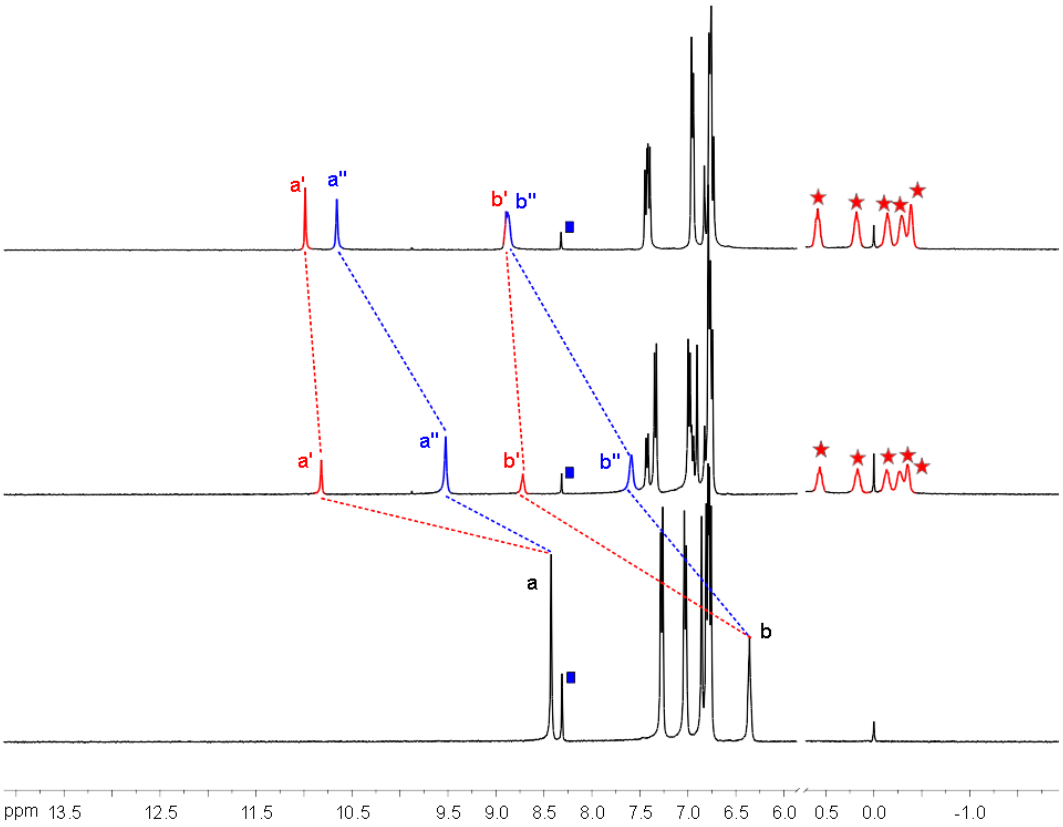

Figure S27. Partial ^{1}H NMR spectra (400 MHz, 298K) of **H** (10 mM) in the presence of increasing amounts of **G20**; from bottom to top: 0.0, 0.8, and 1.5 equivalents. (**a′** and **b′**: signals of urea protons from interpenetrated **H**; **a″** and **b″**: signals of urea protons from non-interpenetrated **H**; ★: signals from methylene protons of encapsulated **G20**; the peaks marked with ■ are ascribed to chloroform)

8. ***Table S1***. The result of ESI-MS analysis on **Gn⊂H**.

Bis-TBA salts of dicarboxylates [**Gn**]	Fomula of **Gn⊂H**	Found [a]	Calculated mass for **Gn⊂H**
Azelate	$C_{104}H_{156}N_6O_{16}$	1502.90 [b]	1502.88 [b]
(**G9**)		630.60 [c]	630.30 [c]
Undecanedioate	$C_{106}H_{160}N_6O_{16}$	1530.90 [b]	1530.91 [b]
(**G11**)		644.45 [c]	644.31 [c]
Dodecanedioate	$C_{107}H_{162}N_6O_{16}$	1545.00 [b]	1544.93 [b]
(**G12**)		651.60 [c]	651.32 [c]
Tridecanedioate	$C_{108}H_{164}N_6O_{16}$	1559.90 [b]	1559.94 [b]
(**G13**)		658.65 [c]	658.83 [c]
Tetradecanedioate	$C_{109}H_{166}N_6O_{16}$	1573.00 [b]	1572.96 [b]
(**G14**)		665.70 [c]	665.34 [c]
Pentadecanedioate	$C_{110}H_{168}N_6O_{16}$	1587.75 [b]	1586.97 [b]
(**G15**)		672.60 [c]	672.34 [c]
Eicosanedioate	$C_{115}H_{178}N_6O_{16}$	1657.85 [b]	1657.05 [b]
(**G20**)		707.60 [c]	707.38 [c]

[a]: negative mode; [b] : [**Gn⊂H**-TBA]$^{-}$; [c]: [**Gn⊂H**-2TBA]$^{2-}$

9. Electrospray ionization mass spectra of ***H*** *with* ***Gn*** *in DMSO-d_6*

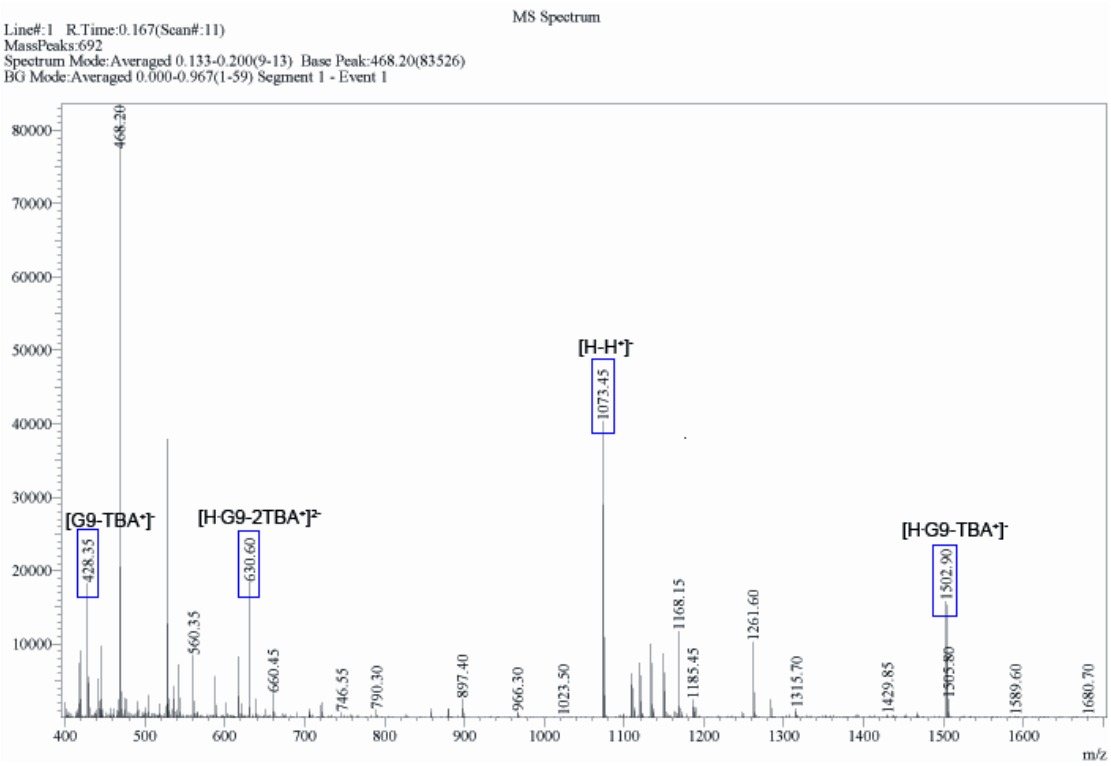

Figure S28. ESI MS of an equimolar DMSO solution of **H** and **G9**.

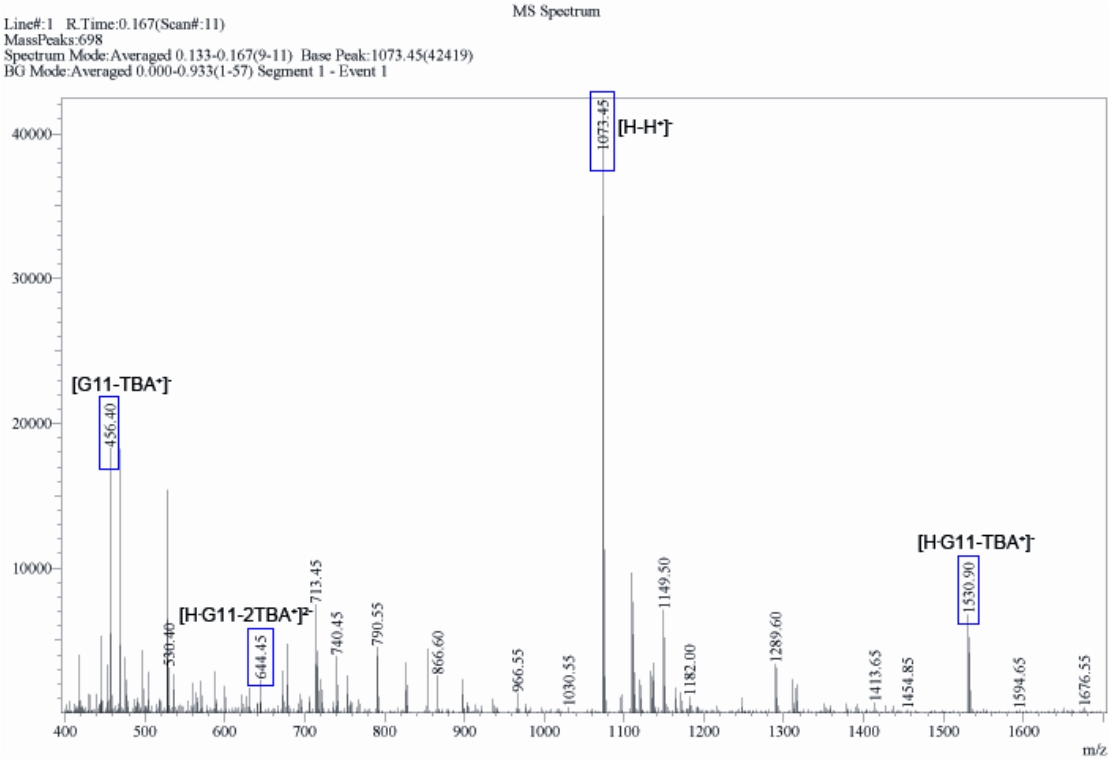

Figure S29. ESI MS of an equimolar DMSO solution of **H** and **G11**.

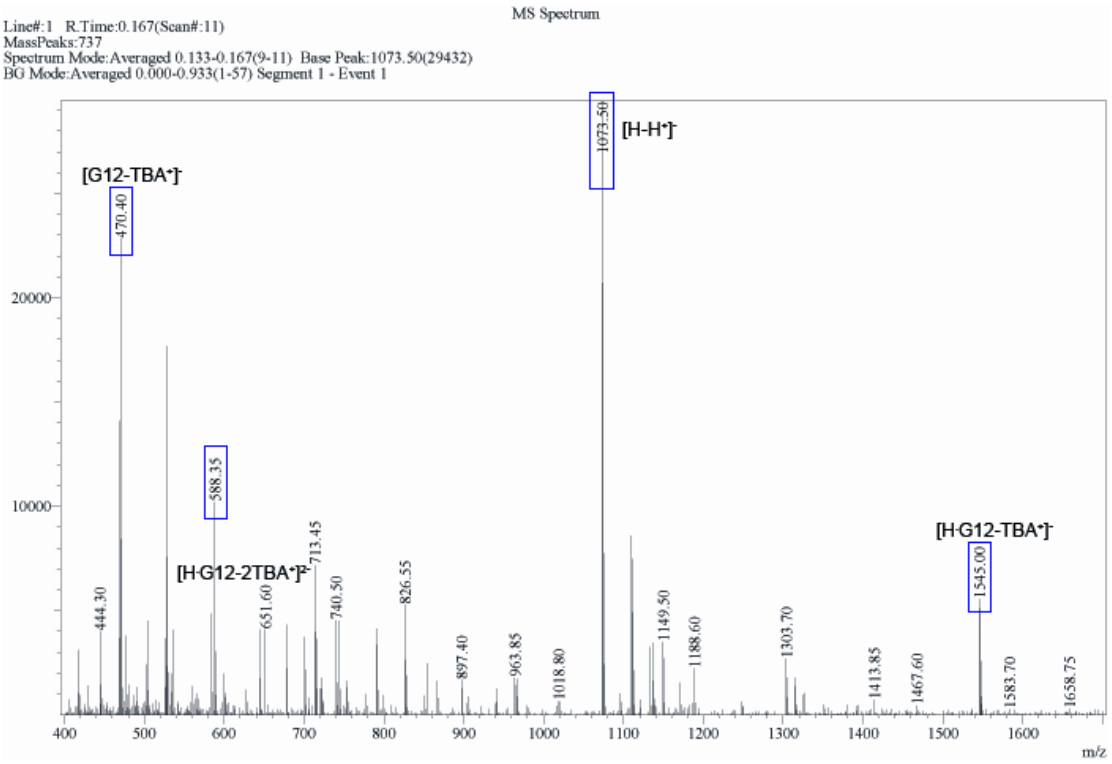

Figure S30. ESI MS of an equimolar DMSO solution of **H** and **G12**.

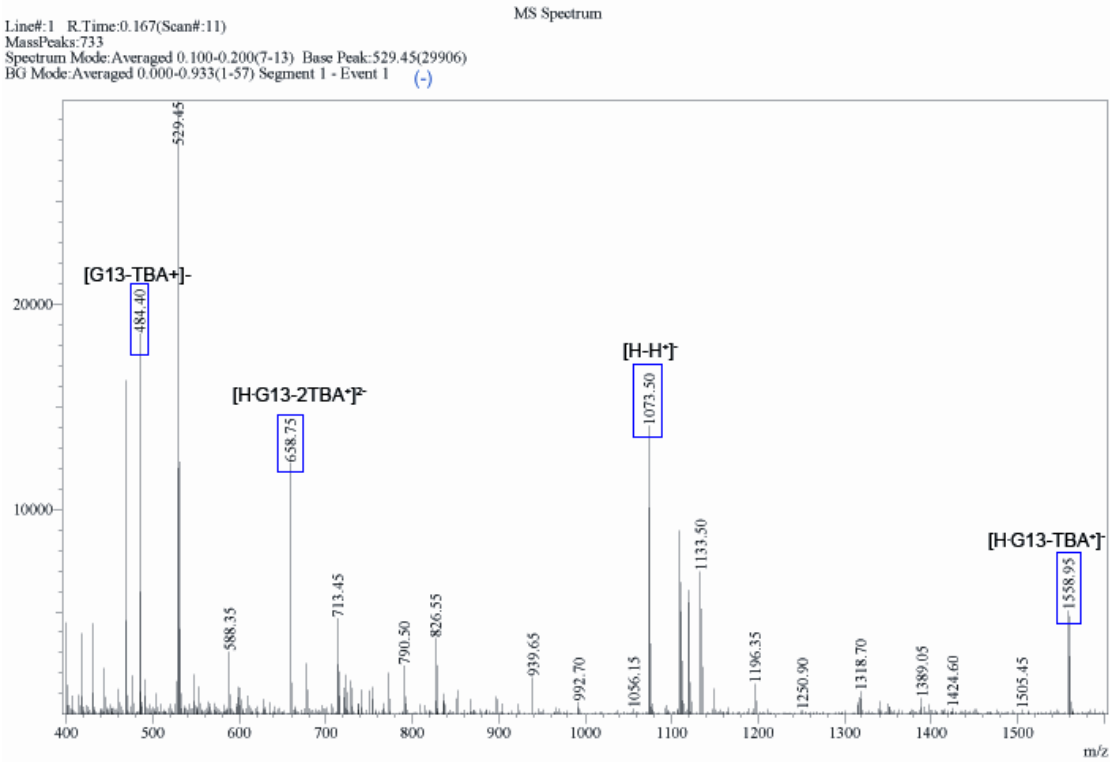

Figure S31. ESI MS of an equimolar DMSO solution of **H** and **G13**.

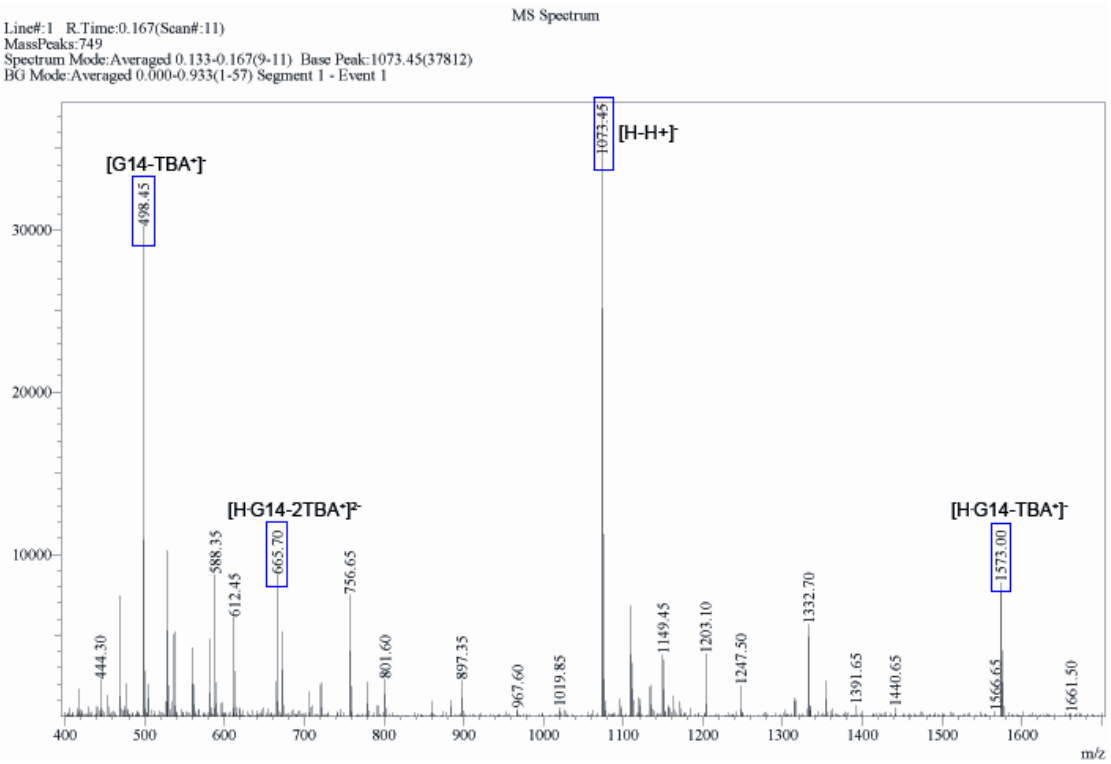

Figure S32. ESI MS of an equimolar DMSO solution of **H** and **G14**.

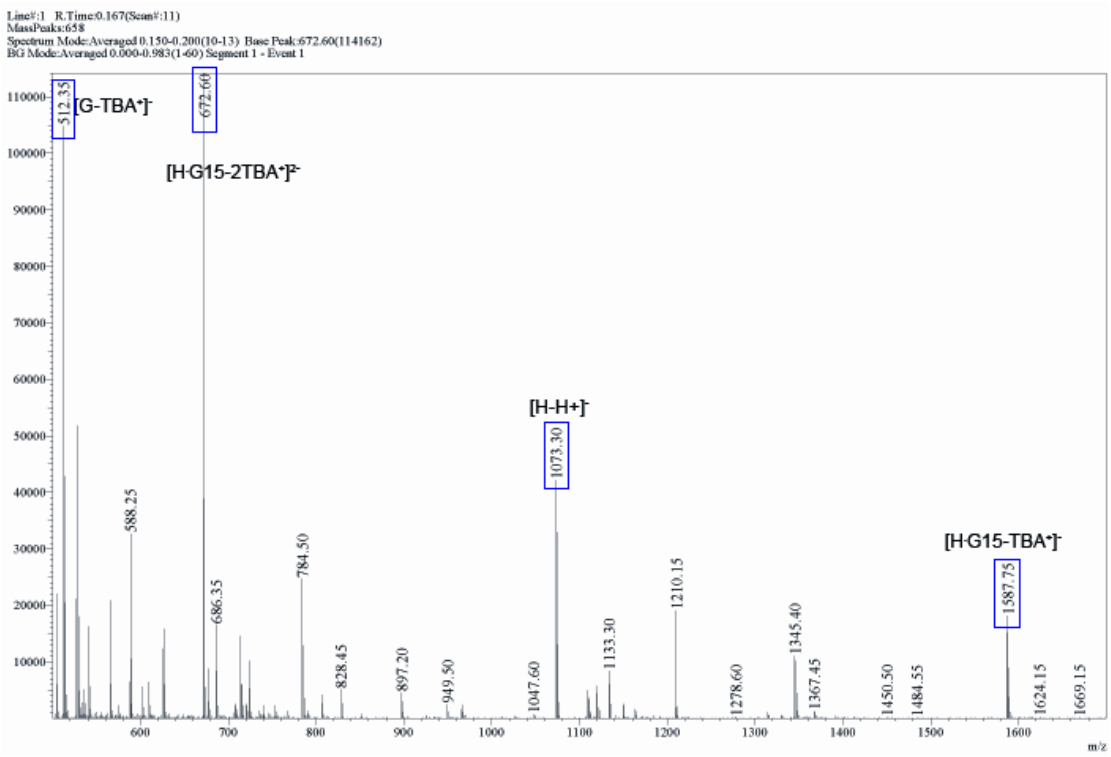

Figure S33. ESI MS of an equimolar DMSO solution of **H** and **G15**.

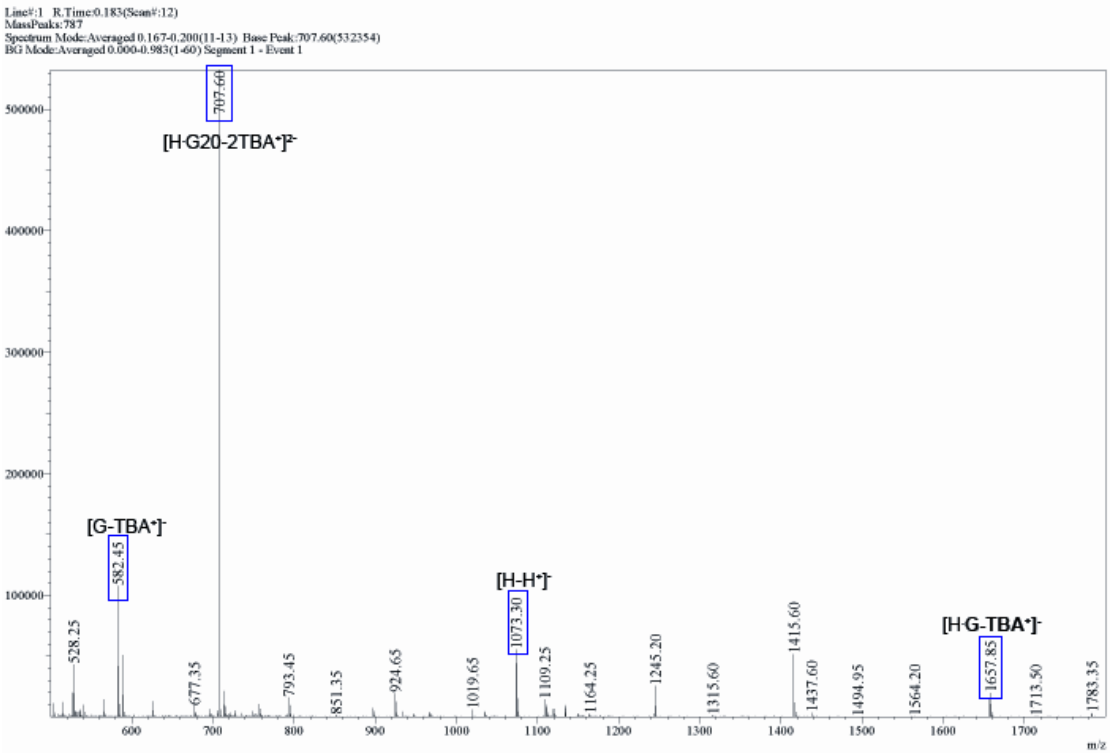

Figure S34. ESI MS of an equimolar DMSO solution of **H** and **G20**.

10. Determination of the association constants.

For **Gn**⊂**H** host-guest complexes, chemical exchange is slow on the NMR time scale and peaks are observed for both pseudorotaxane-type inclusion complexes and external complexes in the NMR spectra. So association constants for pseudorotaxane-type inclusion complexes could be determined by the single-point method[S3] utilizing the following equation and using equal initial concentrations of **H** and **Gn** (10 mM) and the integral values of the urea N*H* resonances (^{1}H NMR spectra) for interpenetrated and non-interpenetrated **H**. (Table 1)

$$K_a = \frac{[\text{pseudorotaxane}]}{[\text{H}]^2_{\text{non-interpenetrated}}}$$

References:

S1. X. Hu, P. Zhang, X. Wu, W. Xia, T. Xiao, J. Jiang, C. Lin and L. Wang, *Polymer Chem*., 2012, DOI: 10.1039/c2py20285a.

S2. B. R. Linton, M. S. Goodman, E. Fan, S. A. van Arman, A. D. Hamilton, *J. Org. Chem.*, 2001, **66**, 7313-7319.

S3. Association constants determined using the ^{1}H NMR single point methods. See: (a) J. C. Adrian, Jr. and C. S. Wilcox, *J. Am. Chem. Soc*., 1991, **113**, 678; (b) S. J. Cantrill, G. J. Youn, J. F. Stoddart and D. J. Williams, *J. Org. Chem*., 2001, **66**, 6857; (c) A. B. Braunschweig, C. M. Ronconi, J.-Y. Han, F. Arico, S. J. Cantrill, J. F. Stoddart, S. I. Khan, A. J. P. White, D. J. Williams, *Eur. J. Org. Chem*., 2006, 1857; (d) S. J. Loeb and J. A. Wisner, *Angew. Chem*., *Int. Ed*., 1998, **37**, 2838–2840; (e) L. Li and G. J. Clarkson, *Org. Lett*., 2007, **9**, 497. (f) C. Li, Q. Xu, J. Li, F. Yao and X. Jia, *Org. Biomol. Chem*., 2010, **8**, 1568; (g) X. Shu, S. Chen, J. Li, Z. Chen, L. Weng, X. Jia and C. Li, *Chem. Commun*., 2012, **48**, 2967